Necessary and Unnecessary Distractor Avoidance Movements Affect User Behaviors in Crossing Operations

SHOTA YAMANAKA, Yahoo Japan Corporation, Japan
WOLFGANG STUERZLINGER, Simon Fraser University, Canada

The "crossing time" to pass between objects in lassoing tasks is predicted by Fitts' law. When an unwanted object, or *obstacle*, intrudes into the user's path, users curve the stroke to avoid hitting that obstacle. We empirically show that, in the presence of an obstacle, modified Fitts models for pointing with obstacle avoidance can significantly improve the prediction accuracy of movement time compared with standard Fitts' law. Yet, we also found that when an object is (only) close to the crossing path, i.e., a *distractor*, users still curve their stroke, even though the object does not intrude. We tested the effects of distractor proximity and length. While the crossing motion is modified by a nearby distractor, our results also identify that overall its effect on crossing times was small, and thus Fitts' law can still be applied safely with distractors.

CCS Concepts: • **Human-centered computing → HCI theory, concepts and models**; **Pointing**; **Empirical studies in HCI**.

Additional Key Words and Phrases: Crossing, pointing, graphical user interface, human motor performance, obstacle avoidance, distractors.

ACM Reference Format:
Shota Yamanaka and Wolfgang Stuerzlinger. 2020. Necessary and Unnecessary Distractor Avoidance Movements Affect User Behaviors in Crossing Operations. *ACM Trans. Comput.-Hum. Interact.* 27, 6, Article 44 (December 2020), 31 pages. https://doi.org/10.1145/3418413

1 INTRODUCTION

Selecting objects is a basic operation in graphical user interfaces. While selecting individual objects is usually easy, selecting groups can be more challenging. For simple groups, shift-clicks or rectangle selection suffice. For selecting complex groups, a commonly offered alternative is lassoing. In this paper, we focus on crossing actions that typically happen in the context of lasso operations.

1.1 Background: Lassoing Operations and its Components

One way to model a lasso operation is by decomposing it into different components, including crossing [38–40]. A *crossing* operation, which passes through a start gate and then an end gate, has been considered as an alternative to traditional *pointing* for selecting a target [2]. Because of its potential lower movement times (MTs)[1] and error rates compared to pointing, the crossing paradigm has attracted the interest of human-computer interaction (HCI) researchers as a means of interaction [2, 5, 37]. Fitts' law [16] predicts the MTs for this task well [1, 2, 5].

[1]As several different notations appear in this article, we summarize them in Appendix A.

Authors' addresses: Shota Yamanaka, syamanak@yahoo-corp.jp, Yahoo Japan Corporation, Tokyo, Japan; Wolfgang Stuerzlinger, w.s@sfu.ca, Simon Fraser University, Vancouver, Canada.

1073-0516/2020/12-ART44 $15.00
https://doi.org/10.1145/3418413

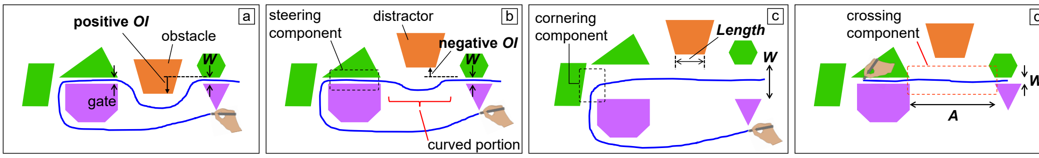

Fig. 1. Lassoing task where users have to pass through a "gate" or "path" bordered by several polygonal objects. (a) Users draw a stroke around the purple objects without hitting other ones. When an (orange) obstacle intrudes into the leftward stroke, users have to curve the stroke downwards. (b) While a distractor does not require a downward-curved stroke, users still tend to do so if the distractor is sufficiently close. (c) However, such curving disappears when the path is wide or the distractor is far. (d) An abstracted crossing task that forms a part of a general lassoing task. In all sub-figures *OI* is the distance of orange distractor from the ideal stroke path, and *Length* is the distance of distractor along the movement direction.

In this paper, we investigate the effect of obstacle and distractor avoidance behaviors — an important element in crossing tasks. Obstacles intrude into the path, while distractors are close to the path (Figure 1). Our motivation is based on the need for predictive models for lasso selection tasks, where users draw a loop around only the intended objects in drawing or illustration software, as shown in Figure 1a. A lasso operation includes several types of component actions such as path-steering and corner-turning in constrained areas (Figure 1b and c). Here we focus on component crossing motions when transitioning between unconstrained and constrained areas (Figure 1d). This corresponds to users trying to pass through a "gate", with width *W* and at a distance *A*, as dictated by the objects surrounding the path.

In our previous work [38–40], we deconstructed a lassoing operation into various components and summed each segment's *MT*s to predict the overall *MT* for a lasso task. If the component models predict the *MT* more accurately than the baseline ones, this modification will increase the prediction accuracy of the resultant, composite model for lassoing time. Still, because a lassoing task includes several complex factors, it is necessary to test candidate models for each component in specific tasks before empirically testing the final, composite model on a lassoing task.

1.2 Motivation: Pilot Study Findings and Distractor Effects on Crossing Strokes

In a pilot study we identified a potential need to take distractor-avoidance behaviors in crossing operations into account. The full description of this pilot can be found in Appendix B. In this pilot, participants had to pass between objects, as in a lassoing task. We identified that a stroke typically curves to safely pass between (distractor) objects, in particular for narrow path widths, as illustrated in Figure 1b. However, we also observed that this behavior disappeared when the width increased, as shown in Figure 1c, likely because there was less danger of hitting undesired objects. Even when curving the stroke was (in theory) unnecessary, user behaviors in unconstrained areas changed depending on the task conditions.

This observation raised the question how user performance in a crossing motion is affected by task conditions, such as the arrangement and shape of non-target (distractor) objects and how these objects change the stroke variability and *MT*. For example, in our pilot study, when the path width increased from 2 to 14 mm, the *MT*s for the curved portion (see Figure 1b) decreased radically from 2522 to 277 msec, and the stroke variability on the y-axis (*SD* of pen tip trajectory) decreased from 5 to 3 mm. We found it interesting that strokes were more curved for a narrower path. This stroke curvature has not been considered in previous work on crossing tasks, because Fitts' law does not assume that users perform such intentional curving. If such curving negatively affects user performance, the predictive accuracy of Fitts' law for the crossing component in a lassoing

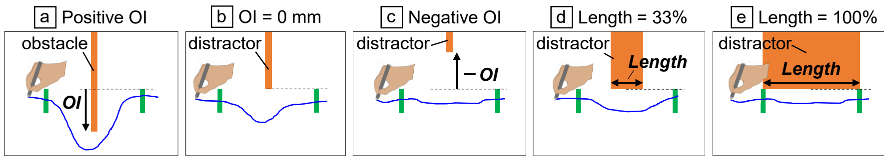

Fig. 2. Parameter definitions for our crossing tasks: obstacle intrusion/distractor distance *OI* and distractor length along the crossing movement *Length*. (a–c) When the *OI* is zero, the bottom edge of the *distractor* is aligned to the top edge of the direct target path. If *OI* is positive, the *obstacle* intrudes into the direct path for crossing motions and thus users have to curve their strokes. If *OI* is negative, intentional curving to avoid the *distractor* is unnecessary. (d and e) The *Length* is defined as the ratio of the movement amplitude *A*.

operation may potentially be degraded. At the same time, improving models for crossing tasks will contribute to improving the overall prediction accuracy of the time for whole lasso operations.

We assume that models of pointing with obstacle avoidance [24, 25, 35], which are modified versions of Fitts' law, are also effective for crossing motions to model *MT*. These models account for a new independent variable called "obstacle/distractor intrusion distance (*OI*)". Yet, these studies have mainly tested *necessary* obstacle avoidance ($OI > 0$, see Figure 2a). However, we observed that strokes were curved even when a distractor was near the direct path, which corresponds to *unnecessary* distractor-avoiding crossing motions for $OI \leq 0$ (Figure 2b and c). Also, those modified models do not consider the size of a distractor along one side of the path, called *Length* (see Figure 2d and e). Hence, an investigation of these conditions is necessary to successfully predict the effects of distractors on crossing times.

1.3 Contribution Statement

- Validating that modified models of pointing with obstacle avoidance can significantly improve the prediction accuracy for *MT* in crossing tasks compared to Fitts' law, when users have to curve their strokes ($OI > 0$). The best-fit model depends on the task type (amplitude or directional constraint).
- Empirically showing that distractors that do not intrude into a crossing path ($OI \leq 0$) and their *Length* significantly affect users' pen stroking motions, in addition to *MT*s and error rates. However, we also show that modified models do not fit the *MT* data substantially better than Fitts' law does for distractors.

We also discuss implications of our work for tasks other than lassoing, including applications involving crossing operations while avoiding non-targets, e.g., *Crossets* [31] or *Bubble Clusters* [36].

2 RELATED WORK

Examples for crossing interfaces in the literature include *CrossY* [4], *Don't click, paint!* [7], *Fold and drop* [12], *Double crossing* [14, 30], *Enhanced area cursors* [15], and *Attribute gates* [34]. Here, we focus on the quantitative aspects of the crossing paradigm, specifically on performance modeling.

2.1 Models for Pointing and Crossing Tasks

The movement time *MT* to point to a target of width *W* at a distance *A* (see Figure 3a) is modeled by Fitts' law [16]:

$$MT = a + b \cdot ID \tag{1}$$

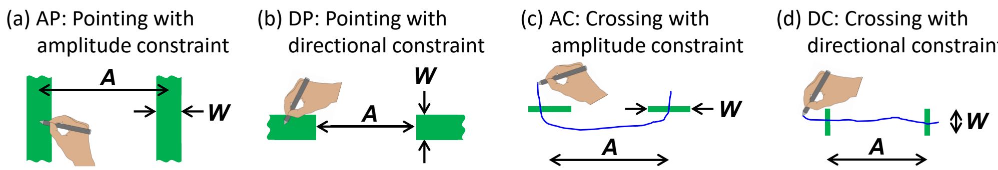

Fig. 3. Comparison of pointing and crossing paradigms with amplitude and directional constraints. In this paper, we denote these crossing task conditions with glyphs: *AC* and *DC*.

where *ID* is the index of difficulty in bits, and a and b are empirically determined regression constants. The original formulation of the *ID* by Fitts (hereafter ID_{Fitts}) is:

$$ID_{\text{Fitts}} = \log_2\left(\frac{2A}{W}\right) \tag{2}$$

In HCI research, the Shannon formulation (ID_{Shannon}) is widely used [29]:

$$ID_{\text{Shannon}} = \log_2\left(\frac{A}{W} + 1\right) \tag{3}$$

The reasoning behind the ID_{Shannon} formulation is well-established [29, 33], and different *ID* formulations have been analyzed from an information-theoretic point of view [20, 23].

Accot and Zhai compared two different pointing tasks using an indirect pen tablet: pointing with an amplitude constraint *AP* (Figure 3a), which is the traditional Fitts' law task, and with a directional constraint *DP* (Figure 3b)[2] [2]. As illustrated in Figure 3c and d, they also investigated crossing with an amplitude constraint *AC* and crossing with a directional constraint *DC*. For all four conditions in Figure 3, the ID_{Shannon} model showed $R^2 > 0.98$ and thus Accot and Zhai concluded that crossing operations are modeled by Fitts' law. Such high correlations were also found for various input devices including direct-input pen tablets [18], touchscreens [28], and mice and trackballs [37].

2.2 Pointing with Obstacle Avoidance

Jax et al. tested the effect of an obstacle in pointing tasks on a 2D surface (Figure 4a) [25]. They used a motion-capturing system to judge if a stroke went over the obstacle. The ID_{Fitts} model showed $R^2 = 0.255$, while adding the *OI* factor significantly improved the fitness with adjusted $R^2 = 0.886$:

$$MT = a + b \cdot (ID_{\text{Fitts}}) + c \cdot (OI) \tag{4}$$

where *OI* is defined as shown in Figure 4c. Vaughan et al. investigated the obstacle effect in 3D space: they used a vertical bar as an obstacle between two target balls as shown in Figure 4b [35]. They tested $OI = -18$, 0, 13, and 25 cm, and proposed the following model:

$$MT = a + b \cdot \log_2\left[\frac{2(A + 2OI)}{W}\right] \tag{5}$$

This model, using $A + 2OI$ as the amplitude for ID_{Fitts} model, was derived based on the three sub-actions participants had to perform: lifting the stylus off for the distance *OI*, moving the target distance *A*, and then homing-in to the target at a distance *OI*. This model showed $R^2 = 0.87$, with no significant difference from Jax et al.'s model with $R^2 = 0.90$ (Equation 4). Due to its smaller number of free parameters, Vaughan et al. thus recommended using Equation 5.

[2]Originally, Accot and Zhai named these conditions "pointing with collinear variability constraint (CP)" and "pointing with orthogonal variability constraint (OP)", respectively. Throughout this paper, we use Apitz et al.'s renaming [5].

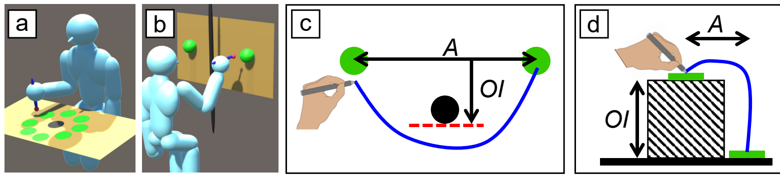

Fig. 4. Pointing task conditions with obstacle avoidance in (a) Jax et al.'s [25] and (b) Vaughan et al.'s [35] work. Task parameters are defined as shown in (c). (d) shows the conditions in Hoffmann and Sheikh's study [24]. Green objects are targets and black ones are obstacles.

Hoffmann and Sheikh's experiment used different heights of targets: the start was on a table and the end target was on a box with height OI [24] (Figure 4d). They proposed the following *two-step model*, which showed $R^2 = 0.96$:

$$MT = a + b \cdot \sqrt{OI} + c \cdot \log_2\left(\frac{2A}{W}\right) \tag{6}$$

The first lifting motion for the distance of OI had no specified area to be aimed for. The MT for such a ballistic motion is modeled as $const \times \sqrt{OI}$ [19]. The second, homing-in phase is modeled by ID_{Fitts}. They then tested a simpler model which assumes that a user aims for the target from the trial beginning, and thus the hand moves smoothly for the distance $A + OI$ without a break. This was termed a *single sweeping motion model*, which showed a fit of $R^2 = 0.92$:

$$MT = a + b \cdot \log_2\left[\frac{2(A + OI)}{W}\right] \tag{7}$$

Because the OI is defined as the "amplitude of the reversible bounce movement" due to the obstacle [35], if the stimulus OI in Figure 4c is negative, the OI can be defined as zero for the purpose of model fitting . Hence, we define the OI used for model fitting here as $\max(0, OI)$.

In these previous studies, a better model was identified by comparing R^2 values, but this approach has been identified as problematic [32]. Because one of our goals is to identify whether we need modified models to predict the MT significantly more accurately than Fitts' law, approaches which penalize additional parameters for determining comparatively better models, such as an adjusted R^2 or the Akaike Information Criterion (AIC) [3], are more appropriate.

In our data analyses, we test the above models of pointing with obstacle avoidance (Equations 4, 5, 6, and 7) and ID_{Shannon} (Equation 3). While these previous studies used the ID_{Fitts} for the final positioning motion, we use the ID_{Shannon} for crossing motions for consistency with existing work on the crossing paradigm. The choice of ID_{Fitts} or ID_{Shannon} has little effect on fitness [20].

3 RESEARCH HYPOTHESES

When a distractor does not intrude into the stroke path ($OI \leq 0$), all candidate models of pointing with obstacle avoidance (Equations 4, 5, 6, and 7) simplify into ID_{Fitts}. This means that the MTs are predicted to be the same value regardless of the values for (negative) OI and *Length*. However, there are several steps needed to validate this hypothesis. We dissect this general hypothesis into research hypotheses (**H1** to **H3**) and address them in Experiments 1–3, respectively.

3.1 H1: When an obstacle intrudes into the path, models of pointing with obstacle avoidance significantly improve the prediction accuracy of *MT* over Fitts' law.

We hypothesize that the modified models of Fitts' law for obstacle avoidance (Equations 4–7) can also be effective for crossing operations. For pointing, these modified models improve model fitness compared with Fitts' law for conditions with obstacles. Also, Fitts' law has proven to fit crossing tasks in the literature. Hence, we test if these models significantly improve the prediction accuracy of MT over Fitts' law for obstacles, i.e., conditions with $OI > 0$ as well.

3.2 H2: Even when a distractor does not intrude into the crossing path, the distance of the distractor can affect the movement time.

As described, the MTs for $OI = -100$ and 0 mm are predicted to be the same according to Equations 4–7, but we question this prediction. Because users typically curve the stroke in the $OI = 0$ mm condition, as we observed in our pilot study, the MT might increase as OI becomes larger, i.e., less negative. If so, formulations other than Equations 4–7 would be needed to improve the fitness significantly.

3.3 H3: Even when a distractor does not intrude into the crossing path, the length of the distractor along the movement direction affects the movement time.

All modified models of pointing with obstacle/distractor avoidance do not consider the *Length* of a distractor in the movement direction, as long as that distractor does not intrude into the path. Yet, our hypothesis is that users should significantly change their MT depending on the *Length*. If so, and similarly to **H2**, models that take distractor *Length* into account should significantly improve the fitness in comparison with Equations 4–7.

4 EXP. 1: EFFECT OF OBSTACLE INTRUSION DISTANCE ON CROSSING TIME

4.1 Participants

We recruited twelve participants, most from a local university (four female, eight male; $M = 23$ years, $SD = 2.1$). All had normal or corrected-to-normal vision and were right-handed. Three participants used pen tablets daily for over a year. Each participant received equivalent to US$ 18.

4.2 Apparatus

We used a direct-input pen tablet, a Sony Vaio Z tablet PC (3.1 GHz Core i7; 16 GB RAM; Windows 10). The display was 13.3 inches, 293.5 × 165.0 mm, at 2560 × 1440 pixels, 0.1146 mm/pixel, with 60 Hz refresh rate. The system read and processed pen-tip input about 125 times per second. The tablet was positioned flat on a table. Participants used the default digitizer stylus pen of the tablet PC (14 cm; 20 g). Finger sensing was disabled when the pen tip contacted the surface, and thus participants were instructed that their palm or fingers could touch the display. The experimental system was implemented with Hot Soup Processor 3.5 and used in full-screen mode.

4.3 Task

The task was to move the pen first through the right green start line and then through the left end line without hitting the orange obstacle/distractor, as shown in Figure 5. When the pen tip contacted the tablet surface, the current position of the pen was shown with a cross-hair cursor, which left a blue trajectory. If the pen was lifted before crossing the end line[3], a friction sound was played and the trial was considered *invalid*. Then, the participants had to re-do *invalid* trials from the start. When a participant hit the obstacle/distractor, a click sound was played and this trial was counted as a hit error ER_{hit}. When an ER_{hit} occurred, the participants still had to finish the trial by crossing the end line. Passing through the outside of the end line was counted as a crossing error ER_{outside}, which played a beep. Even when the participants made such errors (ER_{hit} or ER_{outside}),

[3]Lifting the pen could also be triggered by low pen pressure, tilting the stylus too much, or hardware sensing issues.

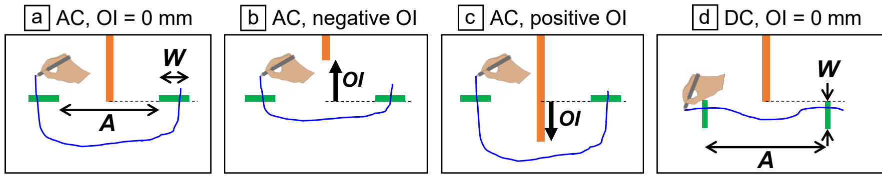

Fig. 5. Definitions of task parameters in Experiment 1.

the trial was judged as *valid*, and participants were not forced to re-do the trial. Participants were instructed to make each stroke as quickly as possible without making errors.

The movement direction was always leftward and the obstacle/distractor was always located above the crossing path; this eliminated the effect of hand occlusion for the end line and obstacle/distractor. The thickness of the obstacle/distractor, start, and end lines was fixed to 3 pixels (0.3 mm), which was the smallest size that ensured visibility. For consistency with previous studies on pointing with obstacle avoidance, the obstacle position on the x-axis was fixed at the midpoint between the start and end lines. The top edge of the obstacle/distractor was always at the top of the display. The top edges of the start and end lines were positioned to be at $1/3^{rd}$ from the top of the display to provide ample room at the bottom of the display area for participants to avoid the obstacle/distractor during their stroke. In the $OI = 0$ mm condition the bottom of the distractor was aligned with the top of the start and end lines for the *DC* condition. More specifically, if the top edge of start and end lines was located at (say) $y = 500$ pixels, the bottom of the distractor was positioned at $y = 499$ pixels. For the *AC* condition, when $OI = 0$ mm, the bottoms of the distractor, start line, and end line were horizontally aligned.

4.4 Design, Procedure, and Measurements

This study used a $4_{OI} \times 3_A \times 2_W$ within-subjects design with the following independent variables and levels: four *OI*s (−10, 0, 10, and 30 mm), three *A*s (50, 80, and 120 mm), and two *W*s (7 and 12 mm). The $OI = 10$ and 30 mm conditions correspond to obstacles, whereas the −10 and 0 mm conditions correspond to distractors. We chose *A*s and *W*s that do not have combinations with a high correlation in terms of ID_{Shannon} (see Appendix C for the motivation). In this first experiment we did not focus on comparing the *task type* (*AC* or *DC*) as an independent variable.

The 12 participants were divided into two groups of 6 persons. One group experienced the *AC* condition first and then *DC*, while the other group saw the opposite order. From the 24 total parameter combinations ($4_{OI} \times 3_A \times 2_W$), 10 conditions were randomly selected as practice trials. After that, each participant performed 5 repetitions of the 24 conditions in random order (= 120 trials). This experiment took approximately 10 minutes. In total, we recorded 120×12 participants = 1440 valid trials for each *AC* or *DC* task, for a grand total of 2880 valid trials.

We measured the following dependent variables: MT, the ER_{hit} rate, and the ER_{outside} rate. The MT was the time spent between the start and end lines. We only analyzed the MT data of error-free trials, as in previous work on the crossing paradigm and pointing with obstacle avoidance.

4.5 Results

We ran a repeated-measures ANOVA in IBM SPSS 24. We used the Bonferroni correction to adjust the p-value to account for multiple comparisons. Throughout this manuscript, in figures showing empirical data, error bars represent 95% confidence intervals, and asterisks indicate significance levels as follows: $^{***}\ p < 0.001$, $^{**}\ p < 0.01$, and $^{*}\ p < 0.05$, as well as n.s. for not significant.

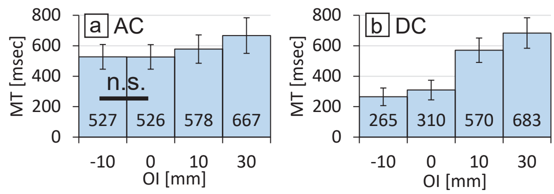

Fig. 6. Effects of *OI* on *MT* in *AC* and *DC* tasks of Experiment 1. Except for a not significant pair ("n.s."), all other pair-wise comparisons showed significant differences (** or ***, i.e., at least $p < 0.01$)[4].

Table 1. ANOVA results for *MT* in Experiment 1.

AC				DC			
Factors	F value	p	η_p^2	Factors	F value	p	η_p^2
OI	$F_{3,33} = 39.571$	***	0.782	OI	$F_{3,33} = 198.802$	***	0.948
A	$F_{2,22} = 138.315$	***	0.926	A	$F_{2,22} = 90.910$	***	0.892
W	$F_{1,11} = 41.552$	***	0.791	W	$F_{1,11} = 49.367$	***	0.818
$OI \times A$	$F_{6,66} = 2.022$	n.s.	0.155	$OI \times A$	$F_{6,66} = 14.339$	***	0.566
$OI \times W$	$F_{3,33} = 2.583$	n.s.	0.190	$OI \times W$	$F_{3,33} = 1.332$	n.s.	0.108
$A \times W$	$F_{2,22} = 6.024$	**	0.354	$A \times W$	$F_{2,22} = 2.192$	n.s.	0.166
$OI \times A \times W$	$F_{6,66} = 1.026$	n.s.	0.085	$OI \times A \times W$	$F_{6,66} = 0.801$	n.s.	0.068

4.5.1 Errors. In total, we recorded 2903 trials, including 23 invalid retrials (0.8%). Among the 2880 valid data points, we observed only one and four obstacle/distractor hits for the *AC* and *DC* conditions, respectively; or 0.07% and 0.3%. Due to the small numbers of obstacle/distractor hits, we found no significant main effects of the task parameters *OI*, *A*, and *W* ($p > 0.05$) on the ER_{hit} rate for both *AC* and *DC* conditions.

We observed 60 and 58 trials where the participants did not cross the end line for the *AC* and *DC* conditions, respectively, which correspond to ER_{outside} rates of 4% and 4%. For the *AC* condition, only *W* significantly affected the ER_{outside} rate: 6% for $W = 7$ mm vs. 2% for $W = 12$ mm ($F_{1,11} = 8.046$, $p < 0.05$, $\eta_p^2 = 0.422$). Similarly, for *DC* only *W* significantly affected the ER_{outside} rate: 6% for $W = 7$ mm vs. 2% for $W = 12$ mm ($F_{1,11} = 14.786$, $p < 0.01$, $\eta_p^2 = 0.573$).

4.5.2 Movement Time. After removing error trials, 2758 data points were analyzed. The mean *MT*s were 575 and 457 msec for the *AC* and *DC* conditions, respectively. ANOVA results are reported in Table 1. For both *AC* and *DC*, the new factor *OI* significantly affected the *MT* with large effect size ($\eta_p^2 > 0.7$). This effect of *OI* on *MT* is shown in Figure 6; the *MT*s tended to increase as *OI* increased. In particular for the *DC* condition, the *MT* for the largest *OI* is more than twice of that for the smallest *OI*. This greater effect of *OI* for the *DC* condition than for *AC* will manifest as different prediction accuracy, even when testing the same model.

4.5.3 Model Fitting. For model fitting of the *AC* condition, we defined the nominal *A* to be the distance between the inside edges of start and end lines (Figure 5). However, when we test model fitness and for consistency with previous work on crossing tasks, we use the length between the centers of the start and end lines, i.e., $A+W$ for the target distance. Thus, $ID_{\text{Shannon}} = \log_2\left(\frac{A+W}{W} + 1\right)$

[4]In this paper, we observed significant differences in pair-wise comparisons where the 95% CIs overlap, such as the *MT*s of $OI = 0$ and 10 mm in Figure 6a. For repeated-measurement experiments, previous work has established that a pair can show significant differences even when 95% CI error bars overlap [10, 13].

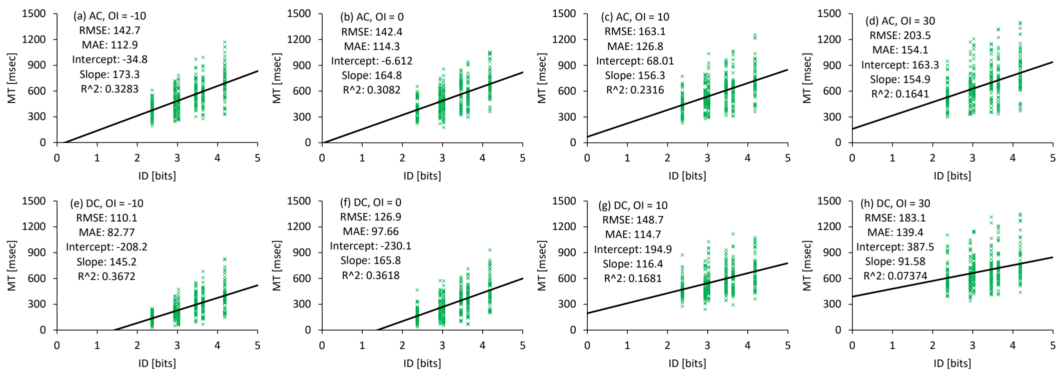

Fig. 7. Scatter plots with all error-free trial data points in Experiment 1, using ID_{Shannon}.

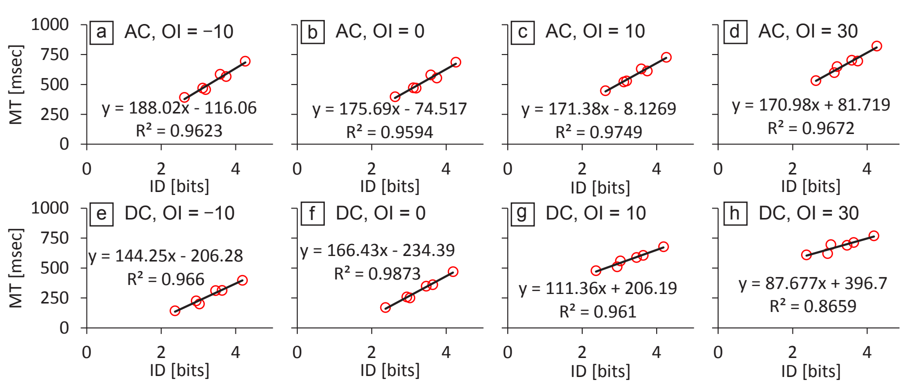

Fig. 8. Model fits for each task type and OI condition in Experiment 1, using ID_{Shannon}.

was applied. Similarly to previous work [2, 24], we also identified only slight differences in the adjusted R^2 values (less than 0.003) with a more realistic amplitude, compared to the nominal A.

There are several methods to report and visualize Fitts' law fitness, such as plotting all trials' data points, using box plots, and plotting the mean data for each participant × condition [26]. First, we show a series of scatter plots for all the error-free trial data in Figure 7. Plotting all data is effective to check for outlier trials or participants and is also helpful for future replication.

Second, Figure 8 illustrates the model fitting results using ID_{Shannon} for $N = 6$ data points $(3_A \times 2_W)$ for each task type and OI condition. Plotting the data this way is a common approach in the Fitts' law literature to check the central tendency [26]. The worst fitness was observed for $DC \times OI = 30$ mm with $R^2 = 0.87$. Similarly to the results of Vaughan et al., using all OI values ($N = 24$) resulted in poorer fits: $R^2 = 0.7013$ and 0.1468 for AC and DC, respectively.

Figure 8 shows that the OI affected mostly the intercept in the AC condition but affected both the slope and intercept in the DC condition. For both AC and DC tasks, even when $A = 0$ mm (i.e., $ID_{\text{Shannon}} = 0$ bits, where the MT shows the intercept), users have to draw a long round-about stroke to avoid the obstacle with $OI = 10$ and 30 mm. Thus, it is inevitable that the MT increased when the OI increased. This is the reason why the intercept changes depending on the OI for both AC and DC. In comparison, the slope indicates the efficiency of the operational style, e.g., mouse vs. touch input [29]. For the DC task with the same ID_{Shannon} value, the MT increased with OI, which had the same effect as when participants used a lower-performance operational

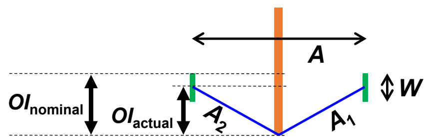

Fig. 9. Definitions of OI_{nominal}, OI_{actual}, A_1, and A_2 for model fitting in the *DC* condition in Experiment 1.

style, because they had to intentionally curve their strokes more. The degree of intentional curving was greater for the *DC* condition than for *AC*, which is also shown in Figure 10. We could also confirm these inconsistent effects of *OI* on the intercepts and slopes statistically as follows. If we regard the *OI* as the independent variable, its effects on the intercept were significant for the *AC* ($F_{3,33} = 15.807$, $p < 0.001$, $\eta_p^2 = 0.590$) and *DC* ($F_{3,33} = 85.713$, $p < 0.001$, $\eta_p^2 = 0.886$) conditions. On the other hand, the effect of *OI* on the slope was not significant for the *AC* ($F_{3,33} = 1.417$, $p = 0.240$, $\eta_p^2 = 0.118$) but significant for *DC* ($F_{3,33} = 18.346$, $p < 0.001$, $\eta_p^2 = 0.625$).

We compared five candidate models, adapted from those proposed in related work. The first is the baseline ID_{Shannon}. The second and third models were proposed by Jax et al. [25] (Equation 4) and Vaughan et al. [35] (Equation 5). Assuming that the central tendency for the crossing position is the center of the target, as in the Fitts paradigm [29], when the nominal *OI* is, e.g., 30 mm and $W = 7$ mm, we use $OI = 30 - (7/2) = 26.5$ mm as the actual *OI* value for model fitting for the *DC* tasks, because the *OI* is defined as the "required bouncing distance" (see Figure 9). Also, we converted $OI = -10$ mm to 0 mm for Equations 4 and 5 for consistency with previous work.

The remaining two models are based on Hoffmann and Sheikh [24] (Equations 6 and 7). The fourth one is their two-step model comprised of ballistic and homing-in phases. For $OI > 0$ mm, the first movement amplitude A_1 is defined as the distance from the center of the start line to the bottom edge of the obstacle, i.e.:

$$A_1 = \sqrt{(OI_{\text{actual}})^2 + (A/2)^2} = \sqrt{(OI_{\text{nominal}} - W/2)^2 + (A/2)^2} \tag{8}$$

By symmetry the second amplitude A_2 is the same as A_1, as shown in Figure 9. For $OI \leq 0$ mm, i.e., distractors, such a step-wise movement would not be required, and thus $A_1 = 0$ mm and $A_2 = A$ in the two-step model (Equation 6). The fifth model is the single sweep movement model (Equation 7), where the total movement distance is:

$$A_1 + A_2 = 2\sqrt{(OI_{\text{nominal}} - W/2)^2 + (A/2)^2} \tag{9}$$

The results of the model fitting using $N = 24$ data points are summarized in Table 2. Because the numbers of regression coefficients are different among the models, we show both the adjusted R^2 and Akaike Information Criterion *AIC* [3, 8] values as indicators of prediction accuracy. As a brief guideline, a model (a) with a lower *AIC* value is a better one, (b) with $AIC \leq (AIC_{\text{minimum}} + 2)$ suggests that it is comparable with better models, and (c) with $AIC \geq (AIC_{\text{minimum}} + 10)$ can be safely rejected. Overall, the baseline model (Equation 3) showed significantly worse fits for both *AC* and *DC* conditions, and modified models of pointing with obstacle avoidance showed significantly better fits in term of *AIC*.

4.6 Discussion

Overall, our results are in line with related work on pointing with obstacle avoidance. For both task types in the *AC* and *DC* conditions, we observed longer *MT*s with larger positive *OI*s (see Figure 6), because participants curved their strokes more to avoid the obstacle. As such intentional curving is more important for the *DC* condition than for *AC*, the difference in *MT* due to *OI*

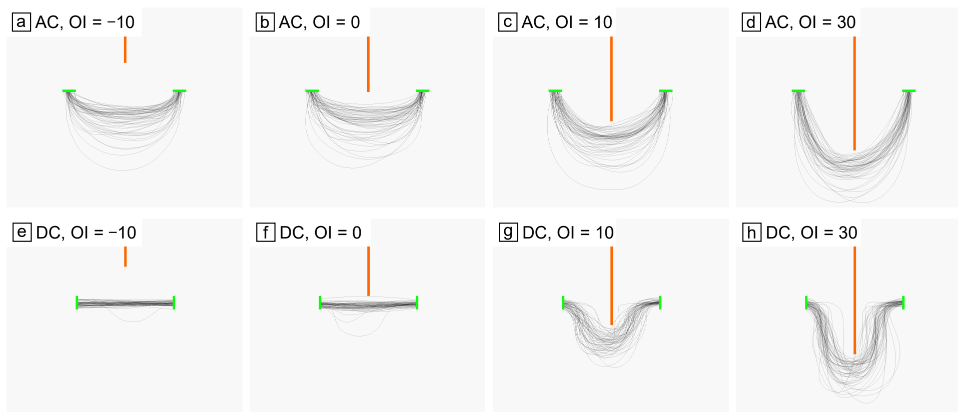

Fig. 10. Pen-tip trajectories from the start to the end line in error-free trials, i.e., the data used for model fitting, for the condition with A = 50 mm × W = 7 mm in Experiment 1. For illustration purposes the start and end lines and distractor are drawn thicker (11 pixels) than the actual value used in the experiment (3 pixels).

Table 2. Model fitting results to predict MT, with adjusted R^2 (higher is better) and AIC (lower is better) for the candidate models. a, b, and c are estimated regression constants with 95% confidence intervals [lower, upper]. Colored cells show the best-fit result for each task type.

Task	Eq.	Model	a	b	c	adj. R^2	AIC
AC	(3) Shannon	$a + b \cdot \log_2\left(\frac{A}{W} + 1\right)$	-29.25 [-205.5, 147.0]	176.5 [125.6, 227.5]	–	0.6877	272.5
	(4) Jax	$a + b \cdot \log_2\left(\frac{A}{W} + 1\right) + c \cdot (OI)$	-75.84 [-130.0, -21.67]	176.5 [161.0, 192.1]	4.660 [4.001, 5.318]	0.9711	216.2
	(5) Vaughan	$a + b \cdot \log_2\left(\frac{A+2(OI)}{W} + 1\right)$	-119.7 [-185.6, -53.90]	189.4 [171.7, 207.2]	–	0.9550	225.9
	(6) Hoffmann (two-part)	$a + b \cdot \sqrt{A_1} + c \cdot \log_2\left(\frac{A_2}{W} + 1\right)$	-72.59 [27.96, 34.06]	31.01 [-135.7, -9.437]	175.4 [157.0, 193.7]	0.9601	224.0
	(7) Hoffmann (sweeping)	$a + b \cdot \log_2\left(\frac{A_1+A_2}{W} + 1\right)$	-122.0 [-248.0, 3.997]	199.1 [163.4, 234.7]	–	0.8528	254.4
DC	(3) Shannon	$a + b \cdot \log_2\left(\frac{A}{W} + 1\right)$	40.56 [-410.2, 491.3]	127.4 [-8.418, 263.3]	–	0.1080	324.4
	(4) Jax	$a + b \cdot \log_2\left(\frac{A}{W} + 1\right) + c \cdot (OI)$	-38.93 [-279.0, 201.2]	117.9 [45.84, 190.0]	14.49 [10.52, 18.46]	0.7504	294.8
	(5) Vaughan	$a + b \cdot \log_2\left(\frac{A+2(OI)}{W} + 1\right)$	-313.0 [-653.2, 27.10]	221.4 [125.1, 317.7]	–	0.4858	311.2
	(6) Hoffmann (two-part)	$a + b \cdot \sqrt{A_1} + c \cdot \log_2\left(\frac{A_2}{W} + 1\right)$	-17.79 [-160.2, 124.6]	59.71 [51.33, 68.09]	95.41 [52.19, 138.6]	0.9073	271.0
	(7) Hoffmann (sweeping)	$a + b \cdot \log_2\left(\frac{A_1+A_2}{W} + 1\right)$	-129.9 [-561.6, 301.8]	175.9 [48.35, 303.5]	–	0.2379	320.7

was larger for DC (see Figure 6), and this resulted in a lower model fitness when using ID_{Shannon} (Equation 3) for the DC condition (adjusted R^2 = 0.1080).

The appropriate model depended on the task type of AC or DC, as supported by the AIC results. As another indication that users exhibit different behaviors depending on the task type, we show all pen-tip trajectories in Figure 10. This shows that, for the AC tasks, the effect of OI on the stroke shape is related to the downward distance. In contrast, for the DC tasks, the stroke shapes can be divided into two different classes. For distractors, i.e., OI = −10 and 0 mm, almost all

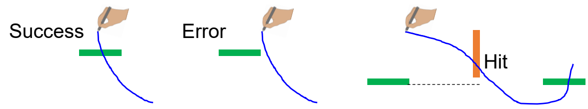

Fig. 11. Passing outside the target is defined as an error. Thus, in the *AC* condition, if users hit a distractor that does not intrude into the crossing path, we always trigger a crossing error.

strokes are linear. Yet, for obstacles, i.e., *OI* = 10 and 30 mm, the participants first passed leftwards through the start line and then sharply curved downwards. This might be one reason why the *MT*s in the *DC* tasks could not be as accurately predicted by a single model as for the *AC* tasks. A possible improvement for the *DC* tasks is to integrate the approach angle towards the target line, as proposed in previous work [5], but this needs further study.

On the basis of the results shown in Table 2, our first hypothesis, **H1: When an obstacle intrudes into the path, models of pointing with obstacle avoidance significantly improve the prediction accuracy of *MT* over Fitts' law**, is supported. That is, when the obstacle intruded into the crossing path, ID_{Shannon} (Equation 3) showed the worst fits for both *AC* and *DC* conditions, and modified models improved the fitness significantly.

While we modeled the *MT* data of *AC* and *DC* conditions separately, the fitness results in Table 2 also indicate that using Equation 6 is in practice the best option when we would like to use a single model for both tasks. Another finding is that, for distractors, i.e., negative or zero *OI* values, we observed a significant difference in *MT*s for the *DC* tasks (Figure 6b). This indicates that, even when a distractor object does not intrude into the path, the *OI* value affects user performance. This motivated us to dig deeper into the details of this behavioral change in Experiments 2 and 3.

5 EXP. 2: EFFECT OF DISTRACTOR OFFSET ON CROSSING TIME

In experiment 2 we investigated only distractors. While Experiments 2 and 3 were logistically conducted on the same day with the same 12 participants, we explain them separately for clarity of exposition. The order of the two experiments was counter-balanced (two groups of six participants). We used the same apparatus as in Experiment 1.

In Experiments 2 and 3, we do not include an *AC* condition. In this condition and after crossing the start line, the cursor keeps on moving downwards, i.e., having downward inertia, and is already away from the distractor's bottom edge. Thus, a distractor that does not intrude into the crossing path can be assumed to not have a strong effect on user behavior. In addition, because a crossing error is defined as passing outside the target line [5, 37], hitting a distractor always means crossing outside of the target (see Figure 11), unless motions that do not conform to our target objectives, such as an 'S' stroke, are involved. Given this, *OI* and *Length* have little expected effect on error-free *MT* data, a fact that is not truly related to the main goal of this part of our work. Consequently, we investigated only conditions equivalent to the *DC* condition in Experiments 2 and 3.

5.1 Participants

We recruited twelve university students (three female, nine male; *M* = 22 years, *SD* = 1.4). All had normal or corrected-to-normal vision and were right-handed. Three participants used pen tablets daily for more than a year. Each participant received the equivalent of US$ 45 for their participation in both experiments. Five of them had also previously participated in Experiment 1[5].

[5]The potential effects of the re-use of participants are analyzed in Appendix D.

5.2 Design

We tested two movement directions: leftward and downward (*Dir* = *Left* and *Down*), where the distractor was located at the top or left side of the ideal path, respectively. These movement directions and distractor positions enable us to avoid potential issues with hand occlusion. We decided to test more than one direction towards our eventual goal of being able to model whole lasso motions. We counter-balanced the order of directions *Dir*, but chose not to analyze it as an independent variable, as this is mostly an ergonomics issue that is outside of our current scope. We placed the tablet in the landscape orientation for *Dir* = *Left* (same as in Experiment 1) and in portrait orientation for *Down* movements. As in Experiment 1, the distractor thickness was 3 pixels (0.3 mm) and the distractor position was the midpoint between the start and end lines. Also, we positioned the midpoint between the start and end lines to be at the center of the tablet display.

This study used a $5_{OI} \times 3_A \times 3_W$ within-subjects design with independent variables of *OI*, *A*, and *W*. We tested five *OI* values: −100, −20, −10, −5, and 0 mm, i.e., only distractors. As *OI* became more negative, the distractor shifted upwards for *Dir* = *Left* and leftwards for *Dir* = *Down*. In the *OI* = −100 mm condition, the distractor was not drawn on the display. For convenience, we define this "no distractor" condition to be equivalent to a −100-mm *OI*, which enables us to uniformly run ANOVA with *OI* as a single independent variable. The second-most negative *OI* of −20 mm was determined based on the work by Kulikov et al., who measured the stroke variability in crossing tasks with a direct-input pen tablet [27]. Their result showed that there were practically no out-of-path movements for the $W = 16.7$ mm condition, if an a-posteriori "path" was defined between the start and end lines. Based on this, if the distractor is $16.7/2 = 8.35$ mm away from the target center line, there is little chance to hit the distractor. Therefore, we used *OI* = −20 mm as the lower limit for the distractor-present condition, which is more than twice 8.35 mm.

We tested three *A*s (50, 110, and 180 mm) and three *W*s (3, 7, and 12 mm). The *W* values were chosen to cover the same range as the *W*s in previous work on lassoing tasks [38], which used 5 to 11 mm. Then, we determined the *A* values as in Experiment 1 (see also Appendix C). Even for the largest *A*, the takeoff space after crossing the end line was 57 mm, which should be sufficient according to previous work [11].

5.3 Procedure

Half of the 12 participants first experienced *Dir* = *Left* and the other *Dir* = *Down*. From the 45 total parameter combinations ($5_{OI} \times 3_A \times 3_W$), 10 conditions were randomly selected as practice trials. After that, each participant performed 5 repetitions of the 45 conditions in random order (= 225 trials). For a single direction, all trials together took approximately 10 minutes. Overall, we recorded 225 × 12 participants = 2700 valid trials for each *Dir*, for a grand total of 5400 trials.

5.4 Measurements

We measured five dependent variables: *MT*, the ER_{hit} rate, the ER_{outside} rate, the average sampled position of the pen tip along the y-axis (Avg_y), and the corresponding standard deviation (SD_y). The Avg_y and SD_y were computed across all n sampled positions between the start and end lines.

$$Avg_y = \frac{1}{n}\sum_{i=1}^{n} y_i \quad \text{and} \quad SD_y = \sqrt{\frac{1}{n}\sum_{i=1}^{n}(y_i - Avg_y)^2} \tag{10}$$

where y_i ($1 \le i \le n$) is the i-th sampled position of the pen-tip trajectory. The origin of Avg_y was set to the center of the target line. A positive Avg_y means downwards on the display for horizontal movements or rightwards for downward strokes. For simplicity of presentation, we use the subscript 'y' for Avg_y and SD_y also for the *Dir* = *Down* condition, where offsets were actually

Table 3. ANOVA results for *MT* in Experiment 2.

Dir = *Left*				*Dir* = *Down*			
Factors	*F* value	*p*	η_p^2	Factors	*F* value	*p*	η_p^2
OI	$F_{4,44} = 7.760$	***	0.414	*OI*	$F_{4,44} = 10.981$	***	0.500
A	$F_{2,22} = 286.818$	***	0.963	*A*	$F_{2,22} = 235.577$	***	0.955
W	$F_{2,22} = 72.880$	***	0.869	*W*	$F_{2,22} = 93.709$	***	0.895
$OI \times A$	$F_{8,88} = 0.534$	n.s.	0.046	$OI \times A$	$F_{8,88} = 1.401$	n.s.	0.133
$OI \times W$	$F_{8,88} = 1.920$	n.s.	0.149	$OI \times W$	$F_{8,88} = 2.149$	**	0.163
$A \times W$	$F_{4,44} = 25.503$	***	0.699	$A \times W$	$F_{4,44} = 14.664$	***	0.571
$OI \times A \times W$	$F_{16,176} = 0.798$	n.s.	0.068	$OI \times A \times W$	$F_{16,176} = 0.802$	n.s.	0.068

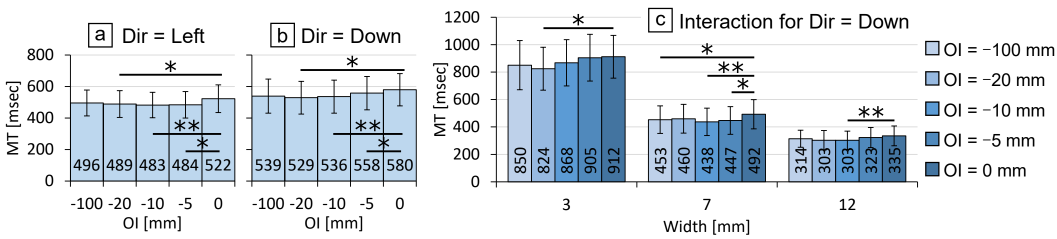

Fig. 12. (a, b) Main effects of *OI* and (c) interaction of $OI \times W$ for *Dir* = *Down* on *MT* in Experiment 2.

horizontal. All Avg_y and SD_y include error trial data to analyze more comprehensively how the participants curved their strokes to avoid the distractor.

5.5 Results

5.5.1 Errors. In total, we recorded 5433 trials, of which 33 were invalid (0.6%). Among the 2700 valid data for each *Dir*, we observed only three and five hits on the distractor for *Dir* = *Left* and *Down*, respectively; or 0.1% and 0.2%. We could not identify significant main effects of the task parameters *OI*, *A*, and *W* ($p > 0.05$) on the ER_{hit} rate for both directions.

For the *Dir* = *Left* condition, we observed 170 trials where the participants missed crossing the end line (6% ER_{outside} rate). The mean ER_{outside} rates were 16, 3, and 0.3% for *W* = 3, 7, and 12 mm, respectively, and pair-wise comparisons showed that the differences were significant ($p < 0.01$) for all *W* pairs. For *Dir* = *Down*, we observed 153 ER_{outside} trials (6%). The mean ER_{outside} rates were 13, 3, and 0.3% for *W* = 3, 7, and 12 mm, respectively, and the differences were significant ($p < 0.01$) for all *W* pairs.

5.5.2 Movement Time. After removing error trials, 2527 and 2544 data points for *Dir* = *Left* and *Down* were analyzed, respectively. The mean *MT*s were 483 and 540 msec for *Dir* = *Left* and *Down*. Although the distractor did not intrude into the ideal crossing path for all *OI* conditions, the *MT*s were significantly affected by *OI* (Table 3). Yet, Figure 12a and b show that the effect of *OI* on the mean *MT* values can only be observed up to a certain point. We originally assumed that *MT* decreases as the *OI* becomes more negative, because users had to pay less and less attention to a distractor increasingly further away. However, for both directions, we did not observe such a monotonic decrease. Although *OI* = 0 mm required significantly longer *MT*s, the negative effect of the distractor on *MT* was not found for a conditions with $OI \leq -5$ mm. Figure 12c shows the significant interaction of *W* and *OI* for *Dir* = *Down*. Only the *OI* = 0 mm condition exhibited a significant difference from the other ones.

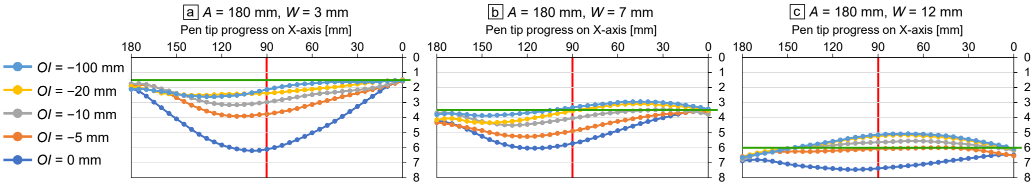

Fig. 13. Averaged trajectory profiles from Experiment 2 for the longest A (180 mm) for Dir = $Left$ including error trials. The origin of the y-axis is aligned to match the top edge of the targets. The scale of the x-axis is 10 times less than the y-axis, which magnifies the y-direction data. The x-y coordinates match the display setting: the strokes start from the right and the distractor (not drawn) is at the top. Each red vertical bar indicates the x-coordinate of the distractor. The green horizontal bars indicate the target center on the y-axis.

5.5.3 Model Fitting. For each $Dir \times OI$ condition, when we ran linear regression for $N = 9$ data points ($3_A \times 3_W$) using ID_{Shannon}, all R^2 values were greater than 0.95. The intercepts and slopes for the five OI conditions are fairly similar for each Dir. Unsurprisingly, the regression for $N = 45$ data points ($5_{OI} \times 3_A \times 3_W$) maintains the prediction accuracy:

$$MT = -527.09 + 249.55 \times ID_{\text{Shannon}}, \quad R^2 = 0.9632 \quad \text{for } Left \tag{11}$$

$$MT = -617.27 + 284.69 \times ID_{\text{Shannon}}, \quad R^2 = 0.9638 \quad \text{for } Down \tag{12}$$

In comparison, in Experiment 1, regressions for each $task\ type \times OI$ condition showed $R^2 > 0.86$ (Figure 8), but using all $N = 24$ data points noticeably degraded the fitness, particularly for DC (adjusted $R^2 = 0.108$, see Table 2). Therefore, in contrast to Experiment 1, we found no benefit to separately predict the MT for each OI value for distractors (that do not intrude into the path).

5.5.4 Trajectory Profile. The mean Avg_y values across all strokes were 0.5 and 0.3 mm for $Dir = Left$ and $Down$, respectively. Table 4 reports the ANOVA results. For both Dir conditions, OI and W had significant main effects on Avg_y. Thus these parameters changed the participants' behavior in terms of how much they avoided the distractor, which is also illustrated in Figure 13. As the raw sample data are very noisy, we re-sampled the trajectory data at 5 mm intervals between the start and end lines in this figure, and calculated the average cursor position on the y-axis.

When the OI was zero, the pen tip trajectory seems to be biased the most away from the origin of the y-axis and thus farther from the bottom edge of the distractor for any W condition, as shown in the blue lines in Figure 13. This is supported by the pair-wise comparisons as shown in Figure 14: the Avg_y values for $OI = 0$ mm condition were larger for all W conditions. Hence, we can state that participants were indeed trying to avoid the distractor when the OI was zero. This avoidance also seems to have induced a greater stroke variability (SD_y) as the OI approached zero (Figure 15).

However, as W increases, the ability to distinguish trajectories for different OI values tends to vanish (Figure 13). This is supported by pair-wise comparisons on SD_y. For $W = 3$ mm, there were significant differences between $OI = 0$ mm and other OI values, as shown in Figure 15. For $W = 7$, there was only a single significantly different pair for $Dir = Down$. For 12 mm, there were no significant differences. Hence, we can statistically confirm that OI and W significantly affected user behaviors on how they curved the stroke, but note that this holds only for small path widths.

5.6 Discussion

Summarizing user behaviours in Experiment 2, the pen tip trajectory curved significantly, particularly when the distractor was close to the ideal path ($OI = 0$ mm) according to the results for Avg_y (Figure 14) and SD_y (Figure 15). Large SD_y values were mainly observed only when the path was

Table 4. ANOVA results for Avg_y in Experiment 2.

Dir = *Left*				*Dir* = *Down*			
Factors	F value	p	η_p^2	Factors	F value	p	η_p^2
OI	$F_{4,44} = 44.407$	***	0.801	OI	$F_{4,44} = 17.935$	***	0.620
A	$F_{2,22} = 0.556$	n.s.	0.048	A	$F_{2,22} = 11.433$	***	0.510
W	$F_{2,22} = 7.351$	**	0.401	W	$F_{2,22} = 10.357$	**	0.485
$OI \times A$	$F_{8,88} = 8.469$	***	0.435	$OI \times A$	$F_{8,88} = 7.658$	***	0.410
$OI \times W$	$F_{8,88} = 1.322$	n.s.	0.107	$OI \times W$	$F_{8,88} = 1.558$	n.s.	0.124
$A \times W$	$F_{4,44} = 8.373$	***	0.432	$A \times W$	$F_{4,44} = 0.901$	n.s.	0.076
$OI \times A \times W$	$F_{16,176} = 1.012$	n.s.	0.084	$OI \times A \times W$	$F_{16,176} = 0.979$	n.s.	0.082

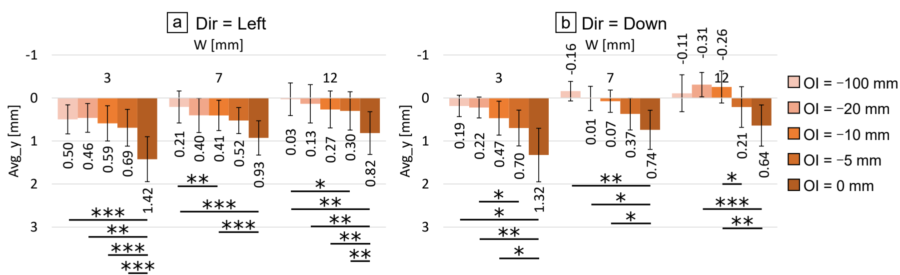

Fig. 14. Averaged pen tip positions on the y-axis in Experiment 2. The origin on the y-axis is aligned to the center of the targets. Positive values on the y-axis correspond to downward movements on the display.

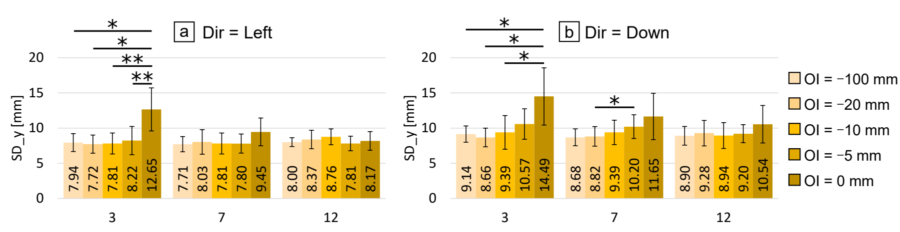

Fig. 15. Standard deviations of the pen tip positions on the y-axis in Experiment 2.

narrow (W = 3 mm, Figure 15). Regarding MTs, conditions where OI = 0 mm and other OI values showed statistical differences, particularly when the path was medium-sized (W = 7 mm, Figure 12). Based on these results, our second hypothesis, **H2: Even when a distractor does not intrude into the crossing path, the distance of the distractor can affect the movement time**, was supported.

However, we observed that the effect of OI on MT was limited. For example, even though the OI value changed from 0 to −100 mm, the change in MT was less than 10%: Figure 12 shows that the largest decrease in MT due to OI was 7% for the *Left* condition, and 9% for *Down*. Also, the effect sizes for OI on MT were small compared with A and W (Table 3). Thus, although our discussions of the outcomes for **H2** are solidly based on the statistical results, we assume that the effectiveness of using $OI < 0$ in modified models for the corresponding tasks is also limited. We will discuss the outcomes in terms of prediction accuracy for potential modified candidate models in Section 7.2 together with the results of Experiment 3.

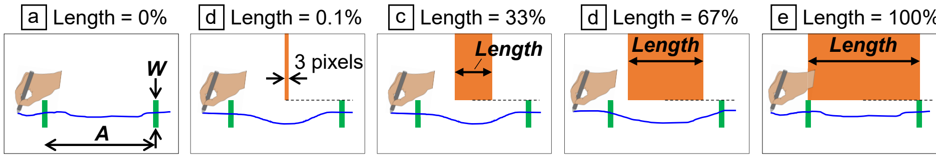

Fig. 16. Task parameter definitions in Experiment 3. If *Length* is 0%, the distractor is absent.

6 EXP. 3: EFFECT OF DISTRACTOR LENGTH ON CROSSING TIME

In this experiment we varied the *Length* of the distractor (see Figure 16). As the *Length* increases, users have to maintain a distance from the distractor for a longer time, thus the *MT* could increase. Yet, when the target is wide, the distance between the ideal path and the distractor increases, and thus the effect of *Length* on *MT* would disappear. We used the same apparatus as in Experiments 1 and 2. As mentioned above, this experiment used the same 12 participants as Experiment 2, in a counter-balanced arrangement.

6.1 Design, Procedure, and Measurements

We used the same values of A and W as in Experiment 2, but this time with five *Lengths*, which resulted in a $5_{Length} \times 3_A \times 3_W$ design. We tested both *Dir* = *Left* and *Down* conditions. The *OI* was fixed to 0 mm. We wanted to explore *Length* values ranging from a minimal one to the full distance between the start and end lines. Thus, we included *Length* = 0, 0.1, 33, 67, and 100%, all as a ratio of the A value. As a baseline, we included a no-distractor condition, which is treated as *Length* = 0% in the ANOVA procedure. The shortest *Length* was set to 0.1%, which rounded up to the thinnest line that was consistently visible on the display: 3 pixels (0.3 mm). The longest value was 100%, which fully covered the movement distance. We also explored mid-range ratios of 33 and 67%.

The entire procedure and measurements were the same as in Experiment 2. The order of *Dir* = *Left* and *Down* was again counter-balanced among the 12 participants. We selected ten conditions from the 45 parameter combinations ($5_{Length} \times 3_A \times 3_W$) as practice trials. Subsequently, each participant performed 5 repetitions of the 45 combinations in random order (225 trials). Overall, we recorded 225 × 12 participants = 2700 valid trials for each *Dir*, for a grand total of 5400 valid trials.

6.2 Results

6.2.1 Errors. Overall, we recorded 5427 trials, including 27 invalid ones (0.5%). We observed 13 and 20 hits of the distractor; 0.5% and 0.7% for the *Dir* = *Left* and *Down* conditions, respectively. Only for *Down*, we observed significant main effects of *Length* ($F_{4,44} = 3.422$, $p < 0.05$, $\eta_p^2 = 0.237$), W ($F_{2,22} = 6.262$, $p < 0.01$, $\eta_p^2 = 0.363$), and $Length \times W$ ($F_{8,88} = 3.650$, $p < 0.05$, $\eta_p^2 = 0.249$) on the ER_{hit} rate. The ER_{hit} rates were 0, 0, 0.9, 0.7, and 2% for *Length* = 0 to 100%, respectively. The ER_{hit} rate decreased as W increased: 2, 0.7, and 0% for W = 3, 7, and 12 mm, respectively, and pair-wise comparisons showed a significant difference between W = 3 and 7 mm ($p < 0.05$). Regarding target misses, we observed 180 ER_{outside} trials (7%) for *Dir* = *Left*, and 145 trials (5%) for *Down*. For *Dir* = *Left*, the ER_{outside} rates were 6, 5, 5, 7, and 10% for *Length* = 0–100%, respectively. For *Dir* = *Down*, the ER_{outside} rates were 5, 6, 6, 5, and 5% for *Length* = 0–100%, respectively.

6.2.2 Movement Time. After removing all error trials, 2513 and 2543 data points for *Dir* = *Left* and *Down*, respectively, remained. The mean *MT*s were 526 and 583 msec for *Dir* = *Left* and *Down*, respectively. ANOVA results are reported in Table 5. We found significant main effects for all independent variables and their interactions, except no interaction of $Length \times A \times W$ for *Dir* = *Left*. Figure 17 shows that the *MT* monotonically increased as *Length* increased for both directions.

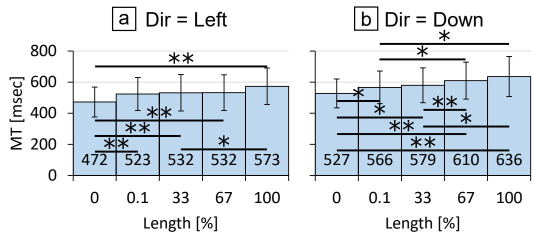

Fig. 17. Main effects of *Length* on *MT* in Experiment 3.

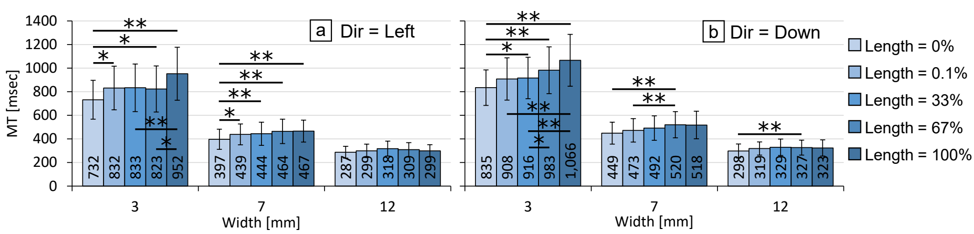

Fig. 18. Interaction of $Length \times W$ on MT in Experiment 3.

Table 5. ANOVA results for *MT* in Experiment 3.

Dir = Left				*Dir = Down*			
Factors	F value	p	η_p^2	Factors	F value	p	η_p^2
Length	$F_{4,44} = 16.953$	***	0.606	*Length*	$F_{4,44} = 17.083$	***	0.608
A	$F_{2,22} = 239.507$	***	0.956	*A*	$F_{2,22} = 154.372$	***	0.933
W	$F_{2,22} = 59.955$	***	0.845	*W*	$F_{2,22} = 90.673$	***	0.892
$Length \times A$	$F_{8,88} = 3.848$	**	0.259	$Length \times A$	$F_{8,88} = 6.413$	***	0.368
$Length \times W$	$F_{8,88} = 10.194$	***	0.481	$Length \times W$	$F_{8,88} = 12.802$	***	0.538
$A \times W$	$F_{4,44} = 28.247$	***	0.720	$A \times W$	$F_{4,44} = 39.554$	***	0.782
$Length \times A \times W$	$F_{16,176} = 1.479$	n.s.	0.119	$Length \times A \times W$	$F_{16,176} = 2.216$	**	0.168

Figure 18 illustrates that the effects of *Length* were more clearly observed for a small W. In contrast to the results of Experiment 2, the *Length* has a comparatively stronger effect on MT. Yet, the effect size of *Length* on MT ($\eta_p^2 \approx 0.6$) is still weaker than that of A ($\eta_p^2 > 0.9$). This could be because the *Length* does not directly increase the necessary movement distance.

6.2.3 Model Fitting. For each $Dir \times Length$ condition, when we ran linear regression for $N = 9$ data points ($3_A \times 3_W$) using ID_{Shannon}, the R^2 values were greater than 0.94. Compared with the results of Experiment 2, the intercepts and slopes for the five *Length* conditions are not that similar. Specifically, the slopes ranged from 237 to 326 msec/bits for $Dir = Left$ and 271 to 369 msec/bits for $Dir = Down$. Thus, regression results using the $N = 45$ data points ($5_{Length} \times 3_A \times 3_W$) showed a slight drop of the prediction accuracy compared with those in Experiment 2:

$$MT = -611.08 + 277.78 \times ID_{\text{Shannon}}, \quad R^2 = 0.9419 \quad \text{for } Left \tag{13}$$

$$MT = -703.00 + 314.24 \times ID_{\text{Shannon}}, \quad R^2 = 0.9430 \quad \text{for } Down \tag{14}$$

In Experiment 3, when approaching the end line, the participants had to avoid moving the pen tip overly upwards for long *Length* conditions. This required a little more attention during the stroke

Table 6. ANOVA results for Avg_y in Experiment 3.

Dir = *Left*				*Dir* = *Down*			
Factors	F value	p	η_p^2	Factors	F value	p	η_p^2
OI	$F_{4,44} = 34.793$	***	0.760	OI	$F_{4,44} = 43.559$	***	0.798
A	$F_{2,22} = 3.382$	n.s.	0.235	A	$F_{2,22} = 65.584$	***	0.856
W	$F_{2,22} = 21.887$	***	0.666	W	$F_{2,22} = 22.251$	***	0.669
$OI \times A$	$F_{8,88} = 12.603$	***	0.534	$OI \times A$	$F_{8,88} = 8.242$	***	0.428
$OI \times W$	$F_{8,88} = 1.766$	n.s.	0.138	$OI \times W$	$F_{8,88} = 2.917$	**	0.210
$A \times W$	$F_{4,44} = 16.184$	***	0.595	$A \times W$	$F_{4,44} = 2.774$	*	0.201
$OI \times A \times W$	$F_{16,176} = 0.553$	n.s.	0.048	$OI \times A \times W$	$F_{16,176} = 2.800$	***	0.203

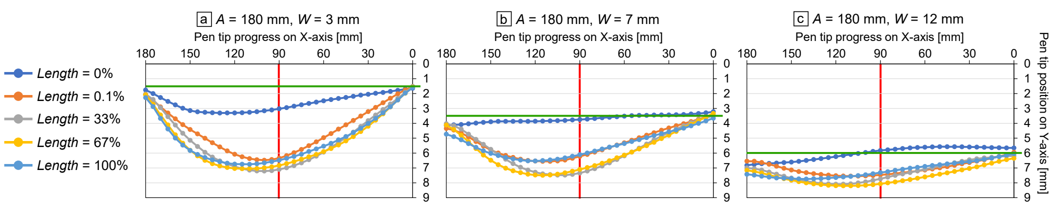

Fig. 19. Averaged trajectory profiles from Experiment 3 for the longest A (180 mm) for *Dir* = *Left* including error trials. The origin of the y-axis is aligned to match the top edge of the targets. The scale of the x-axis is 10 times less than the y-axis, which magnifies the y-direction data. The x-y coordinates match the display setting: the strokes start from the right and the distractor (not drawn) is at the top. Each red vertical bar indicates the x-coordinate of the distractor. The green horizontal bars indicate the target center on the y-axis.

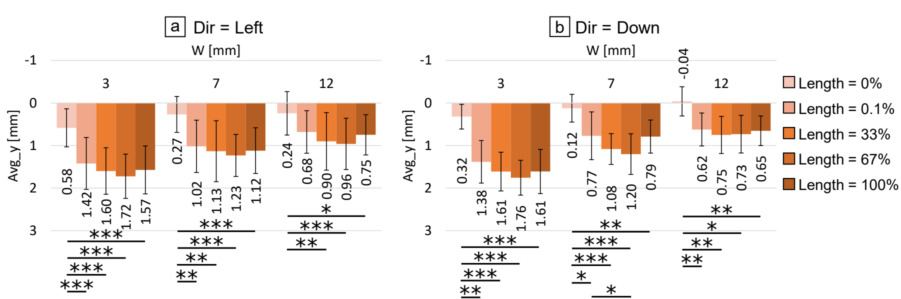

Fig. 20. Averaged pen tip positions on the y-axis for Experiment 3. Positive value on the y-axis signify a downward direction on the display.

compared to Experiment 2, where the 3-pixel-long distractor was always located in the middle of the path. This could have slightly changed intercepts and slopes for different *Length* conditions, and we believe that this is the reason that the overall model fitness was a little lower.

6.2.4 Trajectory Profile. The mean Avg_y values were 1 and 0.9 mm for *Dir* = *Left* and *Down*, respectively. As the ANOVA results reported in Table 6 confirm, the participants significantly curved their strokes depending on the *Length*. Also, for both *Dir* conditions, the Avg_y was significantly affected by W, as the W factor changed the distance from the ideal crossing path to the distractor. These behavioral differences are illustrated in Figure 19.

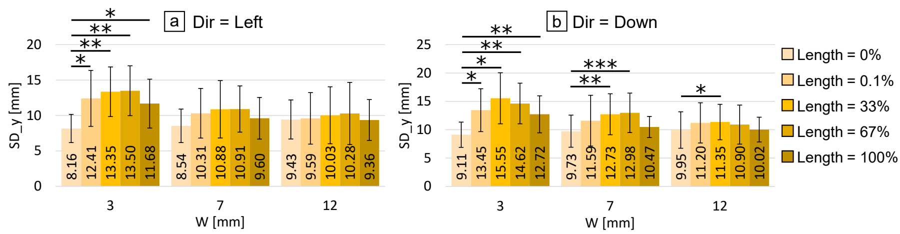

Fig. 21. Standard deviations of pen tip positions on the y-axis in Experiment 3.

Throughout Figure 19a to c, the participants seemed to follow a binary strategy: (1) when *Length* = 0%, the stroke was closer to the target center than in the other *Length* conditions, but (2) the variability in the other four *Length* conditions seems largely to be similar. This was supported by the pair-wise comparisons. As shown in Figure 20, the Avg_y for *Length* = 0% was significantly smaller than in the other conditions for any *W* condition, except for the combination of *Dir* = *Down* × *W* = 7 mm. Also, as shown in Figure 21, significant differences on the SD_y were observed only for conditions with *Length* = 0% for any *W* condition, for both *Dir* conditions. These results identify that, for the *Length* = 0% condition, the stroke was traveling significantly straighter from the start to the end line. Therefore, we can statistically confirm that the participants used an (approximately) binary strategy in terms of the pen tip trajectory, depending on whether the distractor existed or not.

6.3 Discussion

Overall, the effect of longer *Lengths* increasing the *MT* (Figure 17) was more clearly observed in Experiment 3 than the effects of distractor *OI* in Experiment 2. One unexpected result relates to the pen tip trajectory. We assumed that, for a shorter *Length*, such as 3 pixels (*Length* = 0.1%), participants would exhibit only a small curve to temporally avoid the distractor, while they had to continuously avoid the distractor throughout the stroke for *Length* = 100%. However, this assumption has no support, as shown in Figure 19; the participants curved the stroke noticeably even for the shortest (non-zero) *Length* of 0.1%.

Figure 17, which shows the averaged *MT*s for each *Length* value, shows that the largest difference in mean *MT*s for *Dir* = *Left* was 18% and for the *Down* condition was 17%. These differences become greater as the task difficulty increases. For example, for the *Dir* = *Left* condition, at the highest ID_{Shannon} of 5.93 bits, the *MT* for *Length* = 0% was 947 msec and for *Length* = 100% was 1304 msec; this 357 msec difference is 38% of the whole value. Yet, a single regression expression predicts the *MT*s for these conditions as the same value: $MT = -611.08 + 277.78 \times 5.93 = 1036$ msec (Equation 13). From this perspective, modified versions of crossing models that take the *Length* into account have the potential to improve the prediction accuracy (but see Section 7.2).

One positive aspect of this drop in prediction accuracy when using ID_{Shannon} is that, these drops occur only for the worst case scenarios. We tested the full range of *Length* from 0 to 100%, but, e.g., the *MT*s did not increase by (say) twice over the baseline condition even when *Length* = 100%, at least in our experimental conditions. Thus, if we measure a *MT* in a single *Length* condition such as 50%, the *MT*s for other *Length* conditions can be predicted somewhat accurately. This is beneficial for lassoing task *MT* prediction, where various *Length* conditions might exist.

Based on these discussions, **H3: Even when a distractor does not intrude into the crossing path, the length of the distractor along the movement direction affects the movement time**, is supported. Yet, as Figure 18 indicates, this conclusion has limited scope, because the effects of *Length* on *MT* vanished as *W* increased. Thus, the fact that *Length* significantly affected *MT* was confirmed only for small *W* conditions. If we had tested only wide path conditions, such as $W = 15$, 20, and 25 mm, we might have needed to conclude that **H3** was not supported. Also, the effect sizes of *Length* on *MT* were still smaller than those for *A* and *W* (Table 5), and thus we have to (again) assume that the effect of *Length* on model fitting might be limited compared with the overall effect of ID_{Shannon}.

7 GENERAL DISCUSSION

7.1 The Effect of Obstacles and Distractors in Crossing Tasks

In Experiment 1, we identified the first evidence that modified models on pointing with obstacle avoidance could improve the prediction accuracy for crossing tasks with obstacles and distractors. Compared to the *DC* condition, the models worked particularly well for the *AC* condition. We assumed that the reason for this was that the stroke could be performed as a single sweeping motion, as posited by Hoffmann and Sheikh [24] and as shown in Figure 10. On the other hand, for the *DC* conditions, the two-step model still significantly improved the fitness over ID_{Shannon} (Table 2).

The results from Experiment 2 showed that the participants' strokes were significantly affected by a distractor in terms of the distance to the midline (Avg_y) and the curvature (SD_y), see the pen tip trajectory in Figure 13. This indicates that users do change their strategy for how much they curve the stroke around a distractor, depending on its negative *OI*.

In comparison, in Experiment 3, we identified an almost binary strategies depending on when the distractor exists or not; the stroke biases and variability were not dynamically affected by the *Length* values (Figure 19). The effect sizes of *Length* on *MT*s were greater than those for *OI*, and the fitness of ID_{Shannon} was slightly lower in Experiment 3. The effect of *Length* on *MT* was observed specifically for small *W* values (Figure 18). As the *W* increased, significant differences in *MT*s due to *Length* values were observed less, and thus the negative effects of the distractor disappeared.

At the beginning of our work, our original assumptions were:

> Modified models on pointing with obstacle/distractor avoidance estimate the same *MT* value regardless of the *OI* and *Length* if the distractor does not intrude into the crossing path. Yet, intuitively users have to avoid the distractor more as its *OI* increases and *Length* increases. Hence, the *MT*s would significantly change depending on these parameters.

and this assumption was supported, as users changed their strokes according to the task parameters and the *MT*s were significantly affected.

7.2 Model Fitting and Modification Potential

When we analyzed the model fitness in Experiments 2 and 3, we used Fitts' law (i.e., ID_{Shannon}) without including terms for *OI* and *Length*. As above, we converted all negative *OI* values into zero for consistency with previous work. For example, in Vaughan et al.'s work, when the *OI* was negative for the stimulus, the *OI* for model fitting was set to zero and thus their model (Equation 5: $MT = a + b \cdot \log_2[2(A + 2OI)/W]$) became ID_{Fitts}. Also in Experiment 3, there was no "bounce" distance necessary to avoid the distractor, and as no quantitative models that include the *Length* had been developed in previous work, we reported only the fitting results of ID_{Shannon}.

Yet, we empirically observed that these factors significantly affected the *MT*s especially for *Length* for small *W* conditions. Therefore, we examined several possible modifications that use the actual (negative or zero) *OI* for distractors and *Length* values to more accurately model the *MT*s compared to ID_{Shannon}. However, we were not able to identify significant improvements. For

Table 7. Fitting results to predict MT in Experiment 2 ($3_A \times 3_W \times 5_{OI}$ = 45 data points). For models #3, #5, #8, and #10, when $OI = -100$ mm, we use the actual OI distance.

Dir	No.	Model	a	b	c	d	adj. R^2	AIC
Left	#1 (Shannon)	$a + b \cdot \log_2\left(\frac{A}{W}+1\right)$	-527.1	249.6	—	—	0.9632	489.3
	#2 (with-OI_{nominal})	$a + b \cdot \log_2\left(\frac{A}{W}+1\right) + c \cdot (OI)$	-526.4	249.6	0.02723	—	0.9632	491.3
	#3 (with-OI_{actual})	$a + b \cdot \log_2\left(\frac{A}{W}+1\right) + c \cdot (OI)$	-526.1	249.6	0.04734	—	0.9632	491.3
	#4 (inv-OI_{nominal})	$a + b \cdot \left(1 + \frac{c}{d+OI}\right) \cdot \log_2\left(\frac{A}{W}+1\right)$	-527.1	249.0	0.04331	1.426	0.9666	489.0
	#5 (inv-OI_{actual})	$a + b \cdot \left(1 + \frac{c}{d+OI}\right) \cdot \log_2\left(\frac{A}{W}+1\right)$	-527.1	249.0	0.04334	1.429	0.9666	489.0
Down	#6 (Shannon)	$a + b \cdot \log_2\left(\frac{A}{W}+1\right)$	-617.3	284.7	—	—	0.9638	500.5
	#7 (with-OI_{nominal})	$a + b \cdot \log_2\left(\frac{A}{W}+1\right) + c \cdot (OI)$	-611.8	284.7	0.2019	—	0.9644	501.7
	#8 (with-OI_{actual})	$a + b \cdot \log_2\left(\frac{A}{W}+1\right) + c \cdot (OI)$	-611.0	284.8	0.2872	—	0.9645	501.5
	#9 (inv-OI_{nominal})	$a + b \cdot \left(1 + \frac{c}{d+OI}\right) \cdot \log_2\left(\frac{A}{W}+1\right)$	-617.3	279.5	-0.1947	-4.056	0.9677	499.3
	#10 (inv-OI_{actual})	$a + b \cdot \left(1 + \frac{c}{d+OI}\right) \cdot \log_2\left(\frac{A}{W}+1\right)$	-617.3	279.3	-0.2055	-4.227	0.9677	499.3

example, for $Dir = Left$, the ID_{Shannon} model showed an adjusted $R^2 = 0.9632$ and $AIC = 489.3$, see Table 7 (model #1). In a straightforward attempt, we tested an additive factor of OI for the data from Experiment 2:

$$MT = a + b \cdot \log_2\left(\frac{A}{W} + 1\right) + c \cdot (OI), \qquad \text{“with-}OI\text{” model in Table 7} \tag{15}$$

This model using the nominal OI values resulted in adjusted $R^2 = 0.9632$ and $AIC = 491.3$ (model #2 in Table 7), which is not a substantially better fit. If we use the actual distance of the distractor instead of the nominal distance used by the system ($OI = -100$ mm), the difference in adjusted R^2's was less than 0.001 (model #3 in Table 7). Other potential modifications involve different formulations, which have to still obey the overall constraints. For example, while the MT increases as OI becomes more negative, a model must still converge to ID_{Shannon} when the distractor recedes further, i.e., $OI \to -\infty$, which means that the OI inversely affects the MT. Yet, a model with an additional coefficient to incorporate such a term also did not significantly improve the fit, regardless if we use the nominal value of $OI = -100$ mm (model #4 in Table 7) or the actual value (model #5):

$$MT = a + b \cdot \left(1 + \frac{c}{d + OI}\right) \cdot \log_2\left(\frac{A}{W} + 1\right), \qquad \text{“inv-}OI\text{” model in Table 7} \tag{16}$$

This lack of improvements was also observed in the corresponding model fitting for $Dir = Down$ (models #6 to #10 in Table 7). In particular, the positive d values in models #4 and #5 for $Dir = Left$ show that this formulation does not work well because the MT becomes incalculable when the OI equals to $-d$ (which would lead to a division by zero).

We also tested the following straightforward model for Experiment 3 (model #2 in Table 8):

$$MT = a + b \cdot \log_2\left(\frac{A}{W} + 1\right) + c \cdot (Length), \qquad \text{“with-}Length\text{” model in Table 8} \tag{17}$$

where the $Length$ ranged within [0, 100]%. Compared with ID_{Shannon} (#1 in Table 8), we can state that this modified model showed a slightly better fit, but the difference is not statistically significant. In our work we used an absolute percentage $Length = 0.1\%$ for the minimum visible distractor, but even if we used the value relative to A, e.g., 3 pixels = 0.3 mm, which corresponds to 0.688% of $A = 50$ mm, the difference in adjusted R^2 was again less than 0.0001 (model #3). In the same manner

Table 8. Fitting results to predict MT in Experiment 3 ($3_A \times 3_W \times 5_{Length}$ = 45 data points). For models #3, #5, #8, and #10, we use the percentage of *Length* relative to *A*. The others use the absolute *Length*.

Dir	No.	Model	*a*	*b*	*c*	*d*	adj. R^2	*AIC*
Left	#1 (Shannon)	$a + b \cdot \log_2\left(\frac{A}{W} + 1\right)$	-611.1	277.8	—	—	0.9405	520.5
	#2 (with-$Length_{\mathrm{abs}}$)	$a + b \cdot \log_2\left(\frac{A}{W} + 1\right) + c \cdot (Length)$	-638.6	277.8	0.6885	—	0.9475	515.8
	#3 (with-$Length_{\mathrm{rel}}$)	$a + b \cdot \log_2\left(\frac{A}{W} + 1\right) + c \cdot (Length)$	-638.9	277.8	0.6911	—	0.9476	515.8
	#4 (inv-$Length_{\mathrm{abs}}$)	$a + b \cdot \left(1 + \frac{c}{d+Length}\right) \cdot \log_2\left(\frac{A}{W} + 1\right)$	-608.2	297.7	-5.993	61.69	0.9526	515.4
	#5 (inv-$Length_{\mathrm{rel}}$)	$a + b \cdot \left(1 + \frac{c}{d+Length}\right) \cdot \log_2\left(\frac{A}{W} + 1\right)$	-614.5	283.9	-0.009292	0.1304	0.9543	513.7
Down	#6 (Shannon)	$a + b \cdot \log_2\left(\frac{A}{W} + 1\right)$	-703.0	314.2	—	—	0.9417	530.7
	#7 (with-$Length_{\mathrm{abs}}$)	$a + b \cdot \log_2\left(\frac{A}{W} + 1\right) + c \cdot (Length)$	-739.0	314.2	0.9004	—	0.9516	523.3
	#8 (with-$Length_{\mathrm{rel}}$)	$a + b \cdot \log_2\left(\frac{A}{W} + 1\right) + c \cdot (Length)$	-638.9	277.8	0.6911	—	0.9476	515.8
	#9 (inv-$Length_{\mathrm{abs}}$)	$a + b \cdot \left(1 + \frac{c}{d+Length}\right) \cdot \log_2\left(\frac{A}{W} + 1\right)$	-700.7	338.0	-6.047	59.12	0.9575	521.5
	#10 (inv-$Length_{\mathrm{rel}}$)	$a + b \cdot \left(1 + \frac{c}{d+Length}\right) \cdot \log_2\left(\frac{A}{W} + 1\right)$	-704.6	339.1	-5.952	58.05	0.9576	521.4

as for the results of Experiment 2, we also tested models #4 (inverse of absolute percentage of *Length*) and #5 (inverse of relative percentage of *Length*). Even though they involve two additional free parameters, these models showed comparatively better fits than ID_{Shannon}, but the differences were still not significant. This lack of improvements was again found for *Dir* = *Down* (models #6 to #10 in Table 8).

Because ID_{Shannon} showed adjusted $R^2 > 0.96$ and 0.94 in Experiments 2 and 3, respectively, the space to improve fitness through modified models is inherently small. Hence, even if a modified model (typically through additional free parameters) exhibits a greater adjusted R^2 value such as 0.97, the potential for significant improvement in terms of *AIC* is low. In addition, ID_{Shannon} uses only the information of the overall path shape (*A* and *W*), and thus, has quite high utility for predicting *MT* even if there is a distractor right beside the path.

7.3 Interpretation of Negative Intercept in Regressions

In some cases the intercept values are negative in our results. For example, in Figure 8e (a *DC* task with $OI = -10$ mm in Experiment 1), the *MT* is predicted as negative when the ID_{Shannon} is less than about 1.4 bits. Negative intercept has been reported frequently for Fitts' law regressions, including in Fitts and Peterson's pointing tasks [17] and papers on crossing tasks [2, 5, 28, 37] and seems to depend mostly on the gathered data [33]. However, if we had experimentally measured the *MT* for that ID_{Shannon} = 1.4 bits, it might be short but must be greater than 0, e.g., 150 msec. Similarly, if we had measured more *MT* data for low ID_{Shannon}s between 0 to 1.4 bits, those additional data points would need to be above the $MT = 0$ msec line. Then, the regression line tilts clockwise and the intercept will pass above the origin. Therefore, a reason behind the negative intercepts is due to a restricted range of tested ID_{Shannon}s, which is a limitation of our experiment.

Based on this result, if we would like to predict *MT*s outside the investigated ID_{Shannon} range by using the regression line, it is possible that the actual *MT*s would not be close to the predicted *MT*s. However, such ID_{Shannon}s would appear in lassoing tasks as extremely narrow or very wide gates. Thus, further experiments might be needed to validate our conclusion for Experiments 2 and 3 that modified models do not significantly improve the prediction accuracy compared with the ID_{Shannon} model, for low and high ID_{Shannon} values.

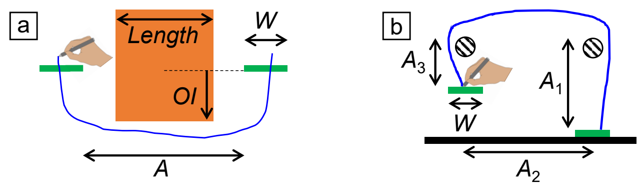

Fig. 22. (a) The *AC* task with a large obstacle intruding into the crossing path. (b) Hoffmann and Sheikh's pointing experiment where there are two obstacles that must be avoided.

7.4 Implications for HCI

It is convenient for the HCI research and practitioner community that *for instances where a distractor does not intrude into a path* we did *not* find evidence for a strong necessity to use different models depending on the distance of that distractor (negative OI) and its *Length*. Therefore, when the distractor does not intrude into the path, using ID_{Shannon} is still the best way to predict the MT. We also reasonably assume that the ID_{Shannon} can be used for conditions where a finite-length distractor is positioned away from the crossing path, e.g., $OI = -10$ mm $\times$ $Length = 50\%$, but this should still be verified in the future.

In contrast, we did not test conditions where an obstacle *intrudes* into the path and has a finite length along the path, as shown in Figure 22a. Here we point out that Hoffmann and Sheikh already investigated pointing with *two-obstacle* avoidance [24]. In that study, participants had to avoid two pegs (obstacles) and then point to the target as shown in Figure 22b. They tested a three-step model that modeled the first and second ballistic motions to avoid the two pegs and the final homing motion, with respective distances A_1, A_2, and A_3:

$$MT = a + b \cdot \sqrt{A_1} + c \cdot \sqrt{A_2} + d \cdot \log_2\left(\frac{2A_3}{W}\right) \tag{18}$$

This model showed $R^2 = 0.88$, but a single-sweeping model of ID_{Fitts} using $A_1 + A_2 + A_3$ for the amplitude still showed $R^2 = 0.94$. Based on this outcome of their study, we assume that the MT for a condition of $OI > 0 \times Length > 0$ could be predicted reasonably better by modified models on pointing with obstacle avoidance.

A more general contribution of our work concerns user interfaces featuring crossing operations. Starting from lassoing operations as the motivating example, our experiments were designed as pure crossing tasks with obstacle/distractor avoidance. Thus, the lessons learned from this work, such as that the MT increases when an obstacle/distractor is located between two targets to be crossed, can also be applied to predicting user performance in other applications. For example, in *Bubble Clusters* [36], *Don't click, paint!* [7], and *Crossets* [31], a user draws a continuous stroke while passing only through the desired targets (icons, toggles and slider knobs, respectively) for selecting multiple targets. During this stroke action, the user must avoid touching unwanted targets; otherwise, the user has to perform another action to un-select the undesired objects or undo the previous selection. While user experiments were conducted in the work on *Bubble Clusters* [36] and *Don't click, paint!* [7], the choices of experimental conditions do not necessarily generalize to all situations that such techniques could be used in. Due to the merit of user performance models, we can, e.g., estimate the potential decrease in task difficulty for a given task when a given technique is used, without conducting additional user studies. In addition to being applicable to other techniques, such as *CrossY* [4] and *Attribute gates* [34], our work will also inform the effectiveness for other, future UIs involving crossing operations.

7.5 Limitations and Future Work

In each of the three experiments, we used twelve university student participants, which represents only a limited sample from the whole user population. Although collecting data from 12 participants is not unusual in the HCI community [9], this sample size is still relatively small and thus a limitation of our study. While we observed sufficient effect sizes for our main results, we acknowledge that if we had collected data from more participants, the results might reveal the differences even better if participants were to use different strategies. For example, if some participants were more careful than those who already joined our experiments, the *MT* differences due to *OI* and *Length* might be more clearly visible.

Our findings are also limited by the experimental conditions tested in our studies, such as the values of A and W used. In addition, we consistently used only a single distractor. Yet, even when there are two or more distractors arranged on both sides of the crossing path at some distance, this still could be classified to fit the $OI \leq 0$ mm condition. Such a task then requires a crossing motion along the middle of the path, and we thus assume that the *MT* increases further. Other untested conditions include a distractor that is placed left- or rightwards from the midpoint between the start and end lines. In our experiments we purposefully tested only conditions where the hand did not occlude the end line nor obstacle/distractor. Yet, in more realistic lassoing tasks the hand could occlude the future path to follow and objects to be selected. Hence, it is necessary to empirically test whether our findings also hold for situations where the hand occludes part of the task.

Additionally, as discussed in Section 7.4, we are interested in the potential interaction of $OI \times Length$. When users need to intentionally avoid a long obstacle ($OI > 0 \times Length > 0$), both factors could affect user performance. However, validating these assumptions requires a task with four independent variables of A, W, *OI*, and *Length*. Because our work is the very first attempt to consider obstacle/distractor-avoidance behavior in crossing operations, we only tested the effects of *OI* and *Length* independently. Yet, as our work showed all of these variables affect user performance, this encourages further experiments with additional variables.

Another untested parameter was the angle of approach to the target. In Experiment 1, the approach angle naturally changed with the *OI* values under the *DC* condition (Figure 10). Also, in Experiments 2 and 3 we found that *OI* and *Length* affected the approach angle, as shown in Figures 13 and 19. Previous work had shown that the approach angle significantly affects the *MT* [5, 6] and therefore it is possible that the angle factor improves model fitness. Still, the space for improvement is relatively small, as discussed above in Section 7.4.

Beyond these limitations, a key contribution is that we bring insights from work on pointing with obstacle avoidance into HCI work on the crossing paradigm and test the applicability of the associated models. We also validated the effects of obstacle avoidance during path traversal in a controlled manner, including statistically sound comparisons of model fitness. Our experiments also identify a space of untested conditions, which informs potential future work.

8 CONCLUSION

As a component of lassoing tasks that select multiple objects through a single stroke, we evaluated the effects of obstacles that intrude into the path of crossing operations and distractors that do not. Before conducting this work, it was unclear if unnecessary curving during a gate-crossing motion, which appear in lassoing operations in illustration software and note-taking tools, affects user performance and the prediction accuracy of Fitts' law. In Experiment 1 where an obstacle intruded into the path, the ID_{Shannon} model showed the worst fit (Table 2), and modified models of pointing with obstacle avoidance significantly improved the fitness for both *AC* and *DC* conditions. In contrast, based on the results of Experiments 2 and 3, the ID_{Shannon} model is a substantially better model to predict the *MT* when there is a distractor that does not intrude into the crossing path, regardless of its *Length* or (negative) *OI*. This outcome is convenient for researchers and practitioners who need to model the *MT* of constrained path-following or lassoing tasks.

To derive an even more general model, we would need to test more conditions, such as the approach angle to the target and distractor positions. Again, the results from Experiments 2 and 3 were obtained for distractors, i.e., conditions where $OI \leq 0$ mm. Investigating the effect of long distractors beside the path ($OI > 0 \times Length > 0$) is one of our next planned steps. To support future modeling efforts, we make our data available online at https://drive.google.com/drive/folders/1b5X-xKgFS_xjfYtzeT_yvjgdf4Nlgb1C?usp=sharing and also in the supplemental material.

Not selecting unintended targets is a common requirement in our daily computer work, but we have little understanding of user behaviors for such operations nor do we have good quantitative models. We believe that our work contributes a series of critical insights for crossing tasks, and that our outcomes will enable future contributions to the HCI field.

A NOTATIONS

As we use several notations in this paper, we summarize them here for the sake of readability.

- ***A***: Movement distance (or amplitude) from the start to the end lines.
- ***W***: Target size (or width), i.e., length of the line that users need to cross.
- ***MT***: Movement time from crossing the start to crossing the end line.
- ***ID***: Index of difficulty of the crossing model, with the same formulation as Fitts' law.
- $\boldsymbol{ID_{\mathrm{Fitts}}}$: Index of difficulty defined by Fitts [16]. $ID_{\mathrm{Fitts}} = \log_2(2A/W)$.
- $\boldsymbol{ID_{\mathrm{Shannon}}}$: Index of difficulty defined by MacKenzie [29]. $ID_{\mathrm{Shannon}} = \log_2(A/W + 1)$.
- ***AP***: Pointing task with amplitude constraint, consisting of two vertical targets.
- ***DP***: Pointing task with directional constraint, consisting of two horizontal targets.
- ***AC***: Crossing task with amplitude constraint, consisting of two horizontal targets.
- ***DC***: Crossing task with directional constraint, consisting of two vertical targets.
- ***OI***: Obstacle intrusion distance. Positive, zero, and negative *OI*s are defined in Figure 2.
- $\boldsymbol{OI_{\mathrm{nominal}}}$: Nominal *OI* defined as an experimental parameter.
- $\boldsymbol{OI_{\mathrm{actual}}}$: Actual *OI* used for model fitting.
- ***Length***: Distractor length along the crossing movement direction, defined as a ratio of *A*.
- $\boldsymbol{ER_{\mathrm{hit}}}$: Operational error of hitting the obstacle or distractor.
- $\boldsymbol{ER_{\mathrm{outside}}}$: Operational error of (not) crossing the target, i.e., users pass outside the target line.
- $\boldsymbol{Avg_y}$: Average pen-tip position along the y-axis during the task from the start to end lines.
- $\boldsymbol{SD_y}$: Standard deviation of the pen-tip trajectory on the y-axis during the task.

B DETAILED RESULTS FOR THE PILOT STUDY

We used the same apparatus as in Experiments 1 to 3 (i.e., a Vaio Z tablet PC). Three unpaid volunteers aged from 25 to 29 (one female and two male) participated, none of which participated in Experiments 1 to 3. All were right-handed and had corrected-to-normal vision. The main goal of our pilot study was to check if the speed formulation of the steering law [22], i.e., the idea that the movement speed is linearly related to the path width *W*, is valid when objects are sparsely arranged and have non-rectangular shapes. The task was to move the pen tip from the left blue area to the right one without hitting the green and purple distractors (Figure 23). The *MT* was measured from when the user exited the start area to entering the end area. The participants were instructed to travel in between without touching any distractors as quickly and accurately as possible. If they hit a distractor, a beep sounded and they had to restart the same condition from the beginning.

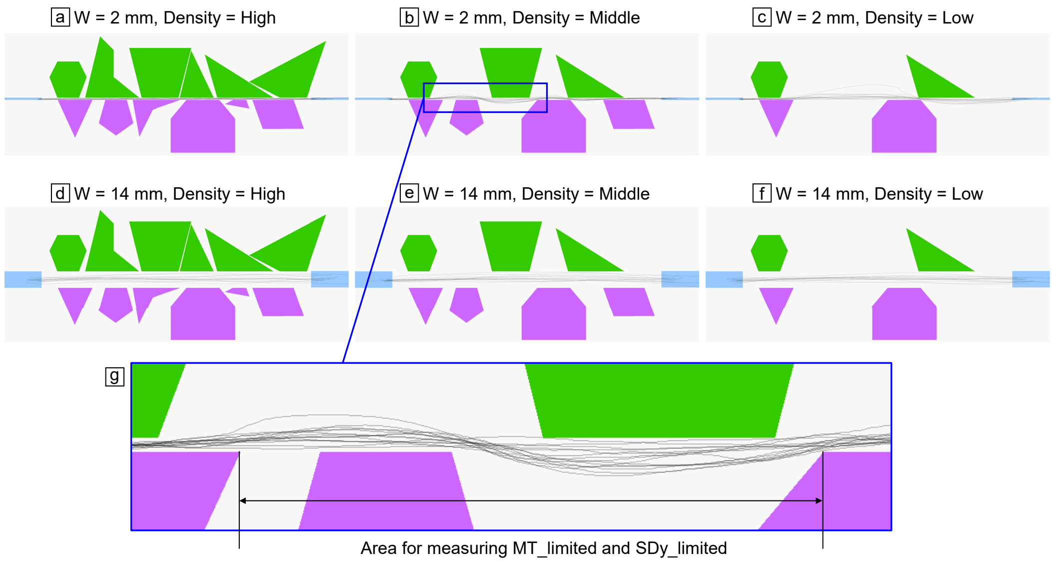

Fig. 23. Object arrangement and example strokes in the pilot study. (a–c) $W = 2$ mm and (d–f) $W = 14$ mm conditions. (g) Enlarged view of a portion of (b) where strokes curve. Each condition includes 15 strokes ($3_{\text{participants}} \times 5_{\text{repetitions}}$).

We prepared three layouts with different distractor densities: *Density* = *High*, *Middle*, and *Low*. The distance between start and end areas was fixed to 230 mm, and the W values were 2, 5, 9, and 14 mm. The participants performed six repetitions of the 12 possible conditions ($3_{Density} \times 4_W$). The first repetition was considered practice, and the remaining five repetitions were used for data-collection. In total, we recorded $3_{\text{participants}} \times 12_{\text{conditions}} \times 5_{\text{repetitions}} = 180$ data points.

We investigated how the unconstrained areas in the *Density* = *Middle* and *Low* conditions affected the participants' strokes. Figure 23 shows that the participants exhibited different strategies depending on the path width. When the path was narrow ($W = 2$ mm), although drawing a straight line can (in theory) accomplish the task, the participants curved their strokes to safely pass between distractors (Figure 23b and c). To show this clearly, we enlarged a part of Figure 23b, as shown in Figure 23g. There it is clearly visible that participants curved some of their strokes to avoid touching distractors, while some strokes still traveled relatively straight. Of course, in the *Density* = *High* condition (Figure 23a), such curving cannot be performed and thus the strokes seem to be comparatively straighter than in *Middle* and *Low*. In contrast, when the path was wide ($W = 14$ mm), we cannot observe such differences in stroke shapes between the *Density* conditions (Figure 23d–f), because the participants did not have to pay attention to the distractors.

We also wanted to investigate how this stroke-curving behavior to avoid hitting distractors affected the operational time. Therefore, we computed the stroke variability and movement time in the limited area shown in Figure 23g. In this portion, i.e., between the end of first purple distractor until the beginning of third purple one in the *Density* = *Middle* condition, the participants had to avoid two distractors (purple pentagon and green trapezoid). These two distractors were absent in the *Density* = *Low* condition, while they were present in the *Density* = *High* condition, where the unconstrained areas were also filled by other distractors. Hence, we chose this portion to identify behavioral differences in stroke variability and time depending on the *Density*.

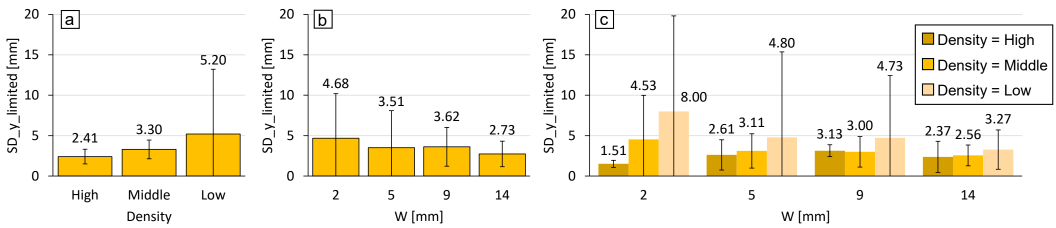

Fig. 24. Effects of $SD_{y_{\text{limited}}}$ in our pilot study.

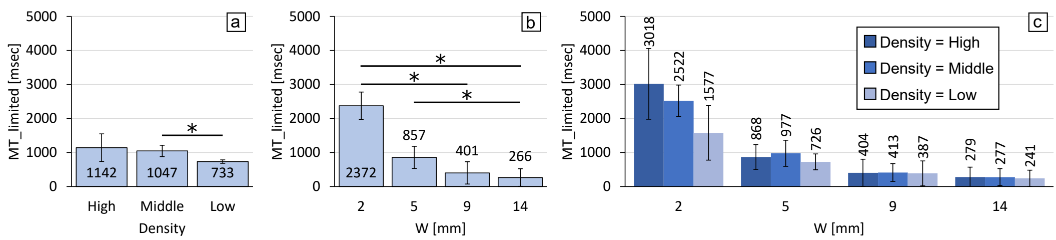

Fig. 25. Effects of MT_{limited} in our pilot study.

Below and for the area annotated in Figure 23g, we call the stroke variability on the y-axis $SD_{y_{\text{limited}}}$, and the time for this portion MT_{limited}:

$SD_{y_{\text{limited}}}$: SD_y in a specific portion of the task, particularly where stroke curving is observed.

MT_{limited}: Movement time in a specific, limited portion of the task, similarly to $SD_{y_{\text{limited}}}$.

We did not find significant main effects of *Density* ($F_{2,4} = 2.096$, $p = 0.238$, $\eta_p^2 = 0.512$) and W ($F_{3,6} = 1.875$, $p = 0.235$, $\eta_p^2 = 0.484$) on $SD_{y_{\text{limited}}}$. Yet, we identified a significant interaction of *Density* $\times$ W ($F_{6,12} = 4.371$, $p < 0.05$, $\eta_p^2 = 0.686$) on $SD_{y_{\text{limited}}}$. Overall, $SD_{y_{\text{limited}}}$ increased as the *Density* decreased (Figure 24a). Interestingly, although larger Ws allow users to draw a stroke with greater variability on the y-axis, $SD_{y_{\text{limited}}}$ actually decreased as the W increased (Figure 24b). As shown in the rightmost three-bar group in Figure 24c, when the path was wide ($W = 14$ mm), $SD_{y_{\text{limited}}}$ values showed small differences for different *Density* conditions. However, for $W = 2$ mm, the *Density* = *Low* condition showed a high $SD_{y_{\text{limited}}}$, although such large curving is (in theory) not necessary. This result indicates that, when the risk to hit distractors was higher, i.e., narrower W conditions, users tried to curve their strokes more if there were more unconstrained areas. Also, the necessity for such intentional curving decreased as W increased in any *Density* condition.

Our final question was how such curving affected the operational time. We found significant main effects of *Density* ($F_{2,4} = 12.913$, $p < 0.05$, $\eta_p^2 = 0.866$) and W ($F_{3,6} = 143.664$, $p < 0.001$, $\eta_p^2 = 0.986$) on MT_{limited}. We also identified a significant interaction of *Density* $\times$ W ($F_{6,12} = 14.014$, $p < 0.001$, $\eta_p^2 = 0.875$) on MT_{limited}. As shown in Figure 25c, when W was 14 mm, the differences in terms of MT_{limited} between the *Density* conditions were small; when W was 2 mm, the participants exhibited faster stroking for lower *Density* conditions.

Comparing the leftmost three bars in Figures 24c and 25c, we noticed that intentional curving with higher $SD_{y_{\text{limited}}}$ did not lengthen the operational time. The likely reason is that a higher *Density* also increases the task difficulty, which thus increases MT_{limited}. Therefore, even though MT_{limited} was affected by *Density* in the $W = 2$ mm condition, it was unclear how intentional stroke-curving ($SD_{y_{\text{limited}}}$) affected MT_{limited}. Hence, we designed the crossing tasks in the main experiments so that we can analyze the effect of stroke curving on operational time in isolation.

C CHOICES OF AMPLITUDE AND WIDTH IN EXPERIMENTS 1 TO 3

As suggested by Gori et al. [21], we checked and confirmed that for each pair of (A, W) that there are no duplicate ID_{Shannon} values. In previous studies, if some (A, W) pairs had the same ID_{Shannon} value, the MTs for that data point were averaged when checking the Fitts' law fitness, e.g., [1]. However, Gori et al. showed that choosing A and W values following a Fitts-like power function design, e.g., $A = 256, 512$, and 1024 mm and $W = 8, 16$, and 32, and then fully crossing these values, incurs the risk of arriving at incorrect conclusions. More specifically, some of these values have the same ID_{Shannon} value such as $(A, W) = (256, 8), (512, 16), (1024, 32)$, and when averaging the MTs for a single ID_{Shannon} data point that comes from different (A, W) pairs, the result can show a misleading high correlation between the ID_{Shannon} and A values, such as R^2 of $(\overline{A}, ID_{\text{Shannon}})$ yielding 0.99 in [1]. Here, if two or more A values provide the same ID_{Shannon} values, those A values are averaged before computing the correlation. Such a high correlation might then lead to the conclusion that "The law X fits to the data well" even if the experimental task is not well-modeled by the law X. The same is also true for averaged W values that have the same ID_{Shannon} values.

The correlations in our parameters are as follows.

- Experiment 1: $(A, W, ID_{\text{Shannon}})$ = (50, 7, 3.03), (50, 12, 2.37), (80, 7, 3.64), (80, 12, 2.94), (120, 7, 4.18), and (120, 12, 3.46). These yield $R^2(\overline{A}, ID_{\text{Shannon}}) = 0.629$ and $R^2(\overline{W}, ID_{\text{Shannon}}) = 0.362$.
- Experiments 2 and 3: $(A, W, ID_{\text{Shannon}})$ = (50, 3, 4.14), (50, 7, 3.03), (50, 12, 2.37), (110, 3, 5.24), (110, 7, 4.06), (110, 12, 3.35), (180, 3, 5.93), (180, 7, 4.74), and (180, 12, 4.00). These yield $R^2(\overline{A}, ID_{\text{Shannon}}) = 0.443$ and $R^2(\overline{W}, ID_{\text{Shannon}}) = 0.651$.

where A and W are in mm, and ID_{Shannon} is in bits. Because our parameters did not have A and W values producing the same ID_{Shannon} values, the $\overline{A}$ value comes from a single value of A when checking correlations, and similarly for W. As a result, the correlations are not as high as in a previous crossing study [1]. Gori et al. discuss also more sophisticated methods to obtain lower correlations between task parameters [21].

D RE-USE OF PARTICIPANTS

Some participants for Experiment 1 also joined Experiments 2 and 3. To investigate if this might have affected our results, we tagged each participant in Experiments 2 and 3 if they had been part of Experiment 1 or not. The post-hoc unpaired two-tailed t-tests (not assuming equal variances) on MT identified no significant effect of participation in Experiment 1 on the results of Experiment 2 nor Experiment 3, regardless of movement direction (all t statistics < 1).

We also found no effects of the order of Experiments 2 and 3 in a post-hoc unpaired two-tailed t-tests (not assuming equal variances) on MT, as follows (again all t statistics < 1). For both directions investigated in Experiment 2, the prior participation in Experiment 3 did not significantly affect the MT. Finally, in Experiment 3, the order had no significant effects for both movement directions. In conclusion, our counter-balancing worked as intended and therefore the issue of shared participants is unlikely to have affected our main results for MT and the model fitting.

REFERENCES

[1] Johnny Accot and Shumin Zhai. 1997. Beyond Fitts' law: models for trajectory-based HCI tasks. In *Proceedings of the SIGCHI Conference on Human Factors in Computing Systems (CHI '97)*. 295–302. https://doi.org/10.1145/258549.258760

[2] Johnny Accot and Shumin Zhai. 2002. More than dotting the i's — foundations for crossing-based interfaces. In *Proceedings of the SIGCHI Conference on Human Factors in Computing Systems (CHI '02)*. 73–80. https://doi.org/10.1145/503376.50339

[3] Hirotugu Akaike. 1974. A new look at the statistical model identification. *IEEE Trans. Automat. Control* 19, 6 (Dec 1974), 716–723. https://doi.org/10.1109/TAC.1974.1100705

[4] Georg Apitz and François Guimbretière. 2004. CrossY: A Crossing-based Drawing Application. In *Proceedings of the 17th Annual ACM Symposium on User Interface Software and Technology (UIST '04)*. ACM, New York, NY, USA, 3–12. https://doi.org/10.1145/1029632.1029635

[5] Georg Apitz, François Guimbretière, and Shumin Zhai. 2008. Foundations for Designing and Evaluating User Interfaces Based on the Crossing Paradigm. *ACM Trans. Comput.-Hum. Interact.* 17, 2, Article 9 (May 2008), 42 pages. https://doi.org/10.1145/1746259.1746263

[6] Caroline Appert, Olivier Chapuis, and Michel Beaudouin-Lafon. 2008. Evaluation of Pointing Performance on Screen Edges. In *Proceedings of the Working Conference on Advanced Visual Interfaces (AVI '08)*. ACM, New York, NY, USA, 119–126. https://doi.org/10.1145/1385569.1385590

[7] Patrick Baudisch. 1998. Don't Click, Paint! Using Toggle Maps to Manipulate Sets of Toggle Switches. In *Proceedings of the 11th Annual ACM Symposium on User Interface Software and Technology (UIST '98)*. ACM, New York, NY, USA, 65–66. https://doi.org/10.1145/288392.288574

[8] Kenneth P. Burnham and David R. Anderson. 2002. *Model selection and multimodel inference: a practical information-theoretic approach* (2 ed.). Springer. 1–488 pages.

[9] Kelly Caine. 2016. Local Standards for Sample Size at CHI. In *Proceedings of the 2016 CHI Conference on Human Factors in Computing Systems (CHI '16)*. Association for Computing Machinery, New York, NY, USA, 981–992. https://doi.org/10.1145/2858036.2858498

[10] Geoff Cumming, Fiona Fidler, and David L. Vaux. 2007. Error bars in experimental biology . *Journal of Cell Biology* 177, 1 (04 2007), 7–11. https://doi.org/10.1083/jcb.200611141

[11] Morgan Dixon, François Guimbretière, and Nicholas Chen. 2008. Optimal Parameters for Efficient Crossing-based Dialog Boxes. In *Proceedings of the SIGCHI Conference on Human Factors in Computing Systems (CHI '08)*. ACM, New York, NY, USA, 1623–1632. https://doi.org/10.1145/1357054.1357307

[12] Pierre Dragicevic. 2004. Combining Crossing-based and Paper-based Interaction Paradigms for Dragging and Dropping Between Overlapping Windows. In *Proceedings of the 17th Annual ACM Symposium on User Interface Software and Technology (UIST '04)*. ACM, New York, NY, USA, 193–196. https://doi.org/10.1145/1029632.1029667

[13] Pierre Dragicevic. 2016. Fair Statistical Communication in HCI. In *Modern Statistical Methods for HCI*. Springer, 291 – 330. https://doi.org/10.1007/978-3-319-26633-6_13

[14] Wenxin Feng, Ming Chen, and Margrit Betke. 2014. Target Reverse Crossing: A Selection Method for Camera-based Mouse-replacement Systems. In *Proceedings of the 7th International Conference on PErvasive Technologies Related to Assistive Environments (PETRA '14)*. ACM, New York, NY, USA, Article 39, 4 pages. https://doi.org/10.1145/2674396.2674443

[15] Leah Findlater, Alex Jansen, Kristen Shinohara, Morgan Dixon, Peter Kamb, Joshua Rakita, and Jacob O. Wobbrock. 2010. Enhanced Area Cursors: Reducing Fine Pointing Demands for People with Motor Impairments. In *Proceedings of the 23Nd Annual ACM Symposium on User Interface Software and Technology (UIST '10)*. ACM, New York, NY, USA, 153–162. https://doi.org/10.1145/1866029.1866055

[16] Paul M. Fitts. 1954. The information capacity of the human motor system in controlling the amplitude of movement. *Journal of Experimental Psychology* 47, 6 (1954), 381–391. https://doi.org/10.1037/h0055392

[17] Paul M. Fitts and James R. Peterson. 1964. Information capacity of discrete motor responses. *Journal of Experimental Psychology* 67, 2 (1964), 103–112. https://doi.org/10.1037/h0045689

[18] Clifton Forlines and Ravin Balakrishnan. 2008. Evaluating Tactile Feedback and Direct vs. Indirect Stylus Input in Pointing and Crossing Selection Tasks. In *Proceedings of the SIGCHI Conference on Human Factors in Computing Systems (CHI '08)*. ACM, New York, NY, USA, 1563–1572. https://doi.org/10.1145/1357054.1357299

[19] Khai-Chung Gan and Errol R. Hoffmann. 1988. Geometrical conditions for ballistic and visually controlled movements. *Ergonomics* 31, 5 (1988), 829–839. https://doi.org/10.1080/00140138808966724

[20] Julien Gori, Olivier Rioul, and Yves Guiard. 2018. Speed-Accuracy Tradeoff: A Formal Information-Theoretic Transmission Scheme (FITTS). *ACM Trans. Comput.-Hum. Interact.* 25, 5, Article Article 27 (Sept. 2018), 33 pages. https://doi.org/10.1145/3231595

[21] Julien Gori, Olivier Rioul, Yves Guiard, and Michel Beaudouin-Lafon. 2018. The Perils of Confounding Factors: How Fitts' Law Experiments Can Lead to False Conclusions. In *Proceedings of the 2018 CHI Conference on Human Factors in Computing Systems (CHI '18)*. Association for Computing Machinery, New York, NY, USA, Article Paper 196, 10 pages. https://doi.org/10.1145/3173574.3173770

[22] Errol R. Hoffmann. 2009. Review of models for restricted-path movements. *International Journal of Industrial Ergonomics* 39, 4 (2009), 578–589. https://doi.org/10.1016/j.ergon.2008.02.007

[23] Errol R. Hoffmann. 2013. Which Version/Variation of Fitts' Law? A Critique of Information-Theory Models. *Journal of Motor Behavior* 45, 3 (2013), 205–215. https://doi.org/10.1080/00222895.2013.778815

[24] Errol R. Hoffmann and Ilyas H. Sheikh. 2012. Goal-directed aimed movements with path obstructions. *Ergonomics* 55, 8 (2012), 946–962. https://doi.org/10.1080/00140139.2012.681809 PMID: 22676580.

[25] Steven A. Jax, David A. Rosenbaum, and Jonathan Vaughan. 2007. Extending Fitts' Law to manual obstacle avoidance. *Experimental Brain Research* 180, 4 (01 Jul 2007), 775–779. https://doi.org/10.1007/s00221-007-0996-y

[26] Alvin Jude, Darren Guinness, and G. Michael Poor. 2016. Reporting and Visualizing Fitts's Law: Dataset, Tools and Methodologies. In *Proceedings of the 2016 CHI Conference Extended Abstracts on Human Factors in Computing Systems (CHI EA '16)*. Association for Computing Machinery, New York, NY, USA, 2519–2525. https://doi.org/10.1145/2851581.2892364

[27] Sergey Kulikov, I. Scott MacKenzie, and Wolfgang Stuerzlinger. 2005. Measuring the Effective Parameters of Steering Motions. In *CHI '05 Extended Abstracts on Human Factors in Computing Systems (CHI EA '05)*. ACM, New York, NY, USA, 1569–1572. https://doi.org/10.1145/1056808.1056968

[28] Yuexing Luo and Daniel Vogel. 2014. Crossing-based Selection with Direct Touch Input. In *Proceedings of the 32Nd Annual ACM Conference on Human Factors in Computing Systems (CHI '14)*. ACM, New York, NY, USA, 2627–2636. https://doi.org/10.1145/2556288.2557397

[29] I. Scott MacKenzie. 1992. Fitts' law as a research and design tool in human-computer interaction. *Human-Computer Interaction* 7, 1 (1992), 91–139. https://doi.org/10.1207/s15327051hci0701_3

[30] Takashi Nakamura, Shin Takahashi, and Jiro Tanaka. 2008. Double-Crossing: A New Interaction Technique for Hand Gesture Interfaces. In *Proceedings of the 8th Asia-Pacific Conference on Computer-Human Interaction (APCHI '08)*. Springer-Verlag, Berlin, Heidelberg, 292–300. https://doi.org/10.1007/978-3-540-70585-7_33

[31] Charles Perin, Pierre Dragicevic, and Jean-Daniel Fekete. 2015. Crossets: Manipulating Multiple Sliders by Crossing. In *Proceedings of the 41st Graphics Interface Conference (GI '15)*. Canadian Information Processing Society, CAN, 233–240.

[32] Seth Roberts and Harold Pashler. 2000. How persuasive is a good fit? A comment on theory testing. *Psychological Review* 107 (04 2000), 358–367. https://doi.org/10.1037//0033-295X.107.2.358

[33] R. William Soukoreff and I. Scott MacKenzie. 2004. Towards a standard for pointing device evaluation, perspectives on 27 years of Fitts' law research in HCI. *International Journal of Human-Computer Studies* 61, 6 (2004), 751–789. https://doi.org/10.1016/j.ijhcs.2004.09.001

[34] Ahmed N. Sulaiman and Patrick Olivier. 2008. Attribute Gates. In *Proceedings of the 21st Annual ACM Symposium on User Interface Software and Technology (UIST '08)*. ACM, New York, NY, USA, 57–66. https://doi.org/10.1145/1449715.1449726

[35] Jonathan Vaughan, Deborah A. Barany, Anthony W. Sali, Steven A. Jax, and David A. Rosenbaum. 2010. Extending Fitts' Law to three-dimensional obstacle-avoidance movements: support for the posture-based motion planning model. *Experimental Brain Research* 207, 1 (01 Nov 2010), 133–138. https://doi.org/10.1007/s00221-010-2431-z

[36] Nayuko Watanabe, Motoi Washida, and Takeo Igarashi. 2007. Bubble Clusters: An Interface for Manipulating Spatial Aggregation of Graphical Objects. In *Proceedings of the 20th Annual ACM Symposium on User Interface Software and Technology (UIST '07)*. Association for Computing Machinery, New York, NY, USA, 173–182. https://doi.org/10.1145/1294211.1294241

[37] Jacob O. Wobbrock and Krzysztof Z. Gajos. 2008. Goal Crossing with Mice and Trackballs for People with Motor Impairments: Performance, Submovements, and Design Directions. *ACM Trans. Access. Comput.* 1, 1, Article 4 (May 2008), 37 pages. https://doi.org/10.1145/1361203.1361207

[38] Shota Yamanaka and Wolfgang Stuerzlinger. 2019. Modeling Fully and Partially Constrained Lasso Movements in a Grid of Icons. In *Proceedings of the 2019 CHI Conference on Human Factors in Computing Systems (CHI '19)*. ACM, New York, NY, USA, Article 120, 12 pages. https://doi.org/10.1145/3290605.3300350

[39] Shota Yamanaka, Wolfgang Stuerzlinger, and Homei Miyashita. 2017. Steering Through Sequential Linear Path Segments. In *Proceedings of the 2017 CHI Conference on Human Factors in Computing Systems (CHI '17)*. ACM, New York, NY, USA, 232–243. https://doi.org/10.1145/3025453.3025836

[40] Shota Yamanaka, Wolfgang Stuerzlinger, and Homei Miyashita. 2018. Steering Through Successive Objects. In *Proceedings of the 2018 CHI Conference on Human Factors in Computing Systems (CHI '18)*. ACM, New York, NY, USA, Article 603, 13 pages. https://doi.org/10.1145/3173574.3174177